Helsinki University of Technology
Materials Physics Laboratory
Espoo 2002

SUPERCONDUCTING PROXIMITY EFFECT IN MESOSCOPIC METALS

Tero Heikkilä

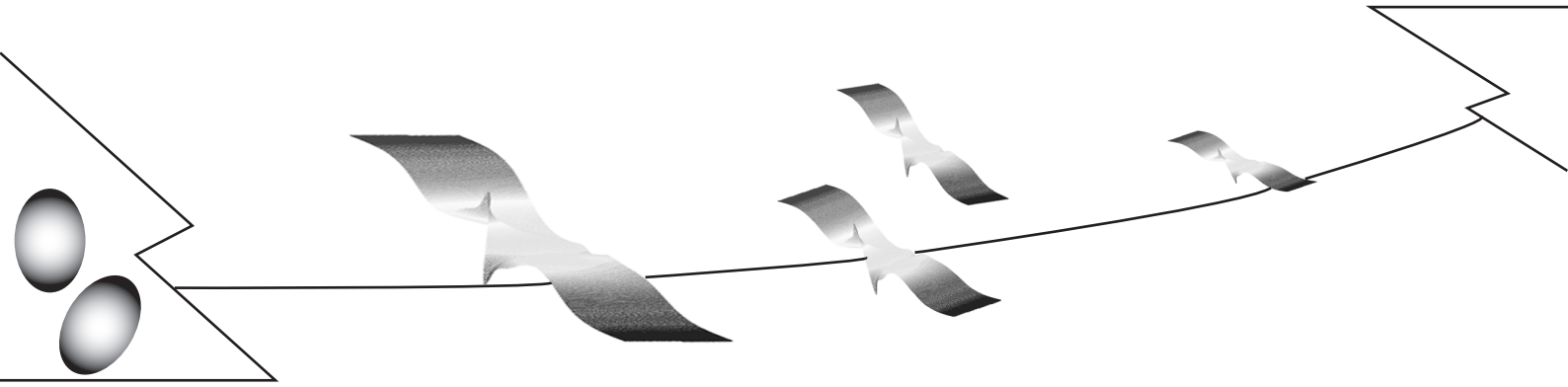

TEKNILLINEN KORKEAKOULU
TEKNISKA HÖGSKOLAN
HELSINKI UNIVERSITY OF TECHNOLOGY
TECHNISCHE UNIVERSITÄT HELSINKI
UNIVERSITE DE TECHNOLOGIE D'HELSINKI

Helsinki University of Technology Publications in Engineering Physics

Teknillisen korkeakoulun teknillisen fysiikan julkaisuja

Espoo 2002 TKK-F-A818

SUPERCONDUCTING PROXIMITY EFFECT IN MESOSCOPIC METALS

Tero Heikkilä

Dissertation for the degree of Doctor of Technology to be presented with due permission for public examination and debate in Auditorium F1 at Helsinki University of Technology (Espoo, Finland) on the 20th of December, 2002, at 12 o'clock noon.

Helsinki University of Technology
Department of Engineering Physics and Mathematics
Materials Physics Laboratory

Teknillinen korkeakoulu
Teknillisen fysiikan ja matematiikan osasto
Materiaalifysiikan laboratorio

Distribution:
Helsinki University of Technology
Materials Physics Laboratory
P.O. Box 2200
FIN-02015 HUT
Tel. +358-9-451-3216
Fax. +358-9-451-3164
E-mail: Tero.T.Heikkila@hut.fi

ISBN 951-22-6187-1
ISSN 1456-3320

Otamedia Oy
Espoo 2002

HELSINKI UNIVERSITY OF TECHNOLOGY
P.O. BOX 1000, FIN-02015 HUT
http://www.hut.fi

ABSTRACT OF DOCTORAL DISSERTATION

Author Heikkilä, Tero Tapio

Name of the dissertation

SUPERCONDUCTING PROXIMITY EFFECT IN MESOSCOPIC METALS

Date of manuscript 28.8.2002 | Date of the disputation 20.12.2002

☐ Monograph ☑ Article dissertation (summary + original articles)

Department Department of Engineering Physics and Mathematics

Laboratory Materials Physics Laboratory

Field of research Theoretical condensed-matter physics

Opponent(s) Prof. Christoph Bruder

Supervisor Prof. Martti M. Salomaa

(Instructors) Prof. Dr. Gerd Schön and Dr. Frank K. Wilhelm

Abstract

The relentless pace for miniaturization of electronic components has reached the limit where quantum-mechanical phenomena can be observed in the currents through submicron-size circuits. In this mesoscopic regime, the conduction electrons exhibit interference effects due to their wave nature, and inelastic scattering ceases to be efficient enough to break the intrinsic phase coherence of the electron waves. In macroscopic metallic wires, such phase-coherent phenomena can be found only in superconducting materials.

This dissertation considers the phenomena encountered in heterostructures of superconductors (S) and mesoscopic normal, nonsuperconducting (N) metals. There, the superconducting order parameter, the pairing amplitude, penetrates into the normal-metal side inducing superconductive features in the normal-metal region near the interface. This superconducting proximity effect alters the properties of the normal metal and makes it possible to transport nondissipative supercurrents through it. An alternative viewpoint is given by the phenomenon of Andreev reflection, which, on the single-particle level, provides the means for the penetration of the pairing amplitude.

Theoretically, SN heterostructures and especially their transport properties can be modelled using two different types of approaches, one based on scattering matrices and the other on quasiclassical Green's functions. In this work, both of these formalisms are utilized in the study of a range of phenomena. These include the mutual proximity effects between superconductors and ferromagnets, the influence of Andreev reflection on universal conductance fluctuations, and nonequilibrium effects in current noise and in supercurrent through normal-metal Josephson weak links.

This study is conducted in a close collaboration with experimental work carried out in different low-temperature laboratories.

Keywords superconductivity, mesoscopics, nanoelectronics, proximity effect, Andreev reflection, Josephson junctions

UDC	538.945:538.935:621.38:539.29	Number of pages	64
ISBN (printed)	951-22-6187-1	ISBN (pdf)	951-22-6186-3
ISBN (others)		ISSN	1456-3320

Publisher Otamedia Oy

Print distribution

☑ The dissertation can be read at http://lib.hut.fi/Diss/

Preface

This work has been carried out in the Materials Physics Laboratory at the Helsinki University of Technology, Finland, and in the Institute for Theoretical Solid State Physics at the University of Karlsruhe, Germany.

I am indebted to Gerd Schön for introducing me to the field of mesoscopics and for the many long discussions where I learned a lot – and not just about physics. I am also grateful to Frank Wilhelm for the numerous discussions – both face to face and by email, for his insightful ideas, and for the friendship through these years. I wish to thank my supervisor Martti Salomaa for giving me the opportunity to work in this field, for the excellent working conditions and for the possibility to connect with the outside world. I am obliged also to my other coauthors, Jochem Baselmans, Norman Birge, Pertti Hakonen, Jian Huang, Teun Klapwijk, Colin Lambert, Rene Lindell, Frédéric Pierre, Mika Sillanpää, Markku Stenberg, Jani Särkkä, Bart van Wees, and Tommy Vänskä for pleasant and fruitful collaboration. I am grateful to Teemu Pohjola for helping me with this manuscript and wish to thank him for his friendship and for the good times both in Finland and in Germany.

I have greatly enjoyed working both in the Materials Physics Laboratory and in the Institute. Besides those already mentioned, I wish to thank for the nice time especially the following people: Tomoya Isoshima, Jouni Knuuttila, Julius Koskela, Saku Lehtonen, Tapani Makkonen, Johanna Meltaus, Mikio Nakahara, Antti Niskanen, Mika Saariaho, Janne Salo, Tapio Simula, Juha Vartiainen, and Sami Virtanen; and Daniel Boese, Fabian Braun, Juan Carlos Cuevas, Mikael Fogelström, Michele Governale, Silvia Kleff, Yuriy Makhlin, Andreas Poenicke, Alexander Shnirman, Andrei Zaikin, and Ulrich Zülicke.

During my Ph.D. work, I have had both the privilege and the pleasure to meet and work with several excellent physicists. In addition to those mentioned above, I thank Jan Aarts, Konstantin Arutyunov, Wolfgang Belzig, Sebastián Bergeret, Yaroslav Blanter, Venkat Chandrasekhar, Hervé Courtois, Pascal Dubos, Rosario Fazio, Jaime Ferrer, Monique Giroud, Frank Hekking, Jani Kivioja, Jonatan Kutchinsky, Jürgen König, Antti Manninen, Achim Marx, Mikko Paalanen, Bernard Pannetier, Jukka Pekola, Roberto Raimondi, R. Seviour, Fabio Taddei, Hideaki Takayanagi, Jussi Toppari, and Anatoli Volkov for enlightening discussions.

Personal scholarships from the Helsinki University of Technology, and the financial support from the Finnish Academy of Science and Letters, the Wihuri foundation, Magnus Ehrnrooth's foundation, Kaupallisten ja Teknillisten Tieteiden Tukisäätiö (KAUTE), Deutsche Akademische Austauschdienst (DAAD), and the European Union program "Superconducting circuits" are gratefully acknowledged. The Center for Scientific Computing (CSC) is acknowledged for excellent computing resources.

I want to express my warmest thanks to my dear wife Mari and lovely daughter Silja for support and good behavior, respectively.

Espoo, August, 2002

Tero Heikkilä

List of Publications

This thesis is a review of the author's work in the field of superconducting proximity effect on phase-coherent metals. It consists of an overview and the following selection of the author's publications in this field:

I. Tero T. Heikkilä, Martti M. Salomaa, and Colin J. Lambert, *Superconducting proximity effect and universal conductance fluctuations*, Phys. Rev. B **60**, 9291 (1999).

II. Markku P. Stenberg and Tero T. Heikkilä, *Nonlinear shot noise in mesoscopic diffusive normal-superconducting systems*, Phys. Rev. B **66**, 144504 (2002).

III. Tero T. Heikkilä, Markku P. Stenberg, Martti M. Salomaa, and Colin J. Lambert, *Thermopower in mesoscopic normal-superconducting structures*, Physica B **284-8**, 1862 (2000).

IV. Mika A. Sillanpää, Tero T. Heikkilä, Rene K. Lindell, and Pertti J. Hakonen, *Inverse proximity effect in superconductors near ferromagnetic material*, Europhys. Lett. **56**, 590 (2001).

V. Tero T. Heikkilä, Frank K. Wilhelm, and Gerd Schön, *Non-equilibrium supercurrent through mesoscopic ferromagnetic weak links*, Europhys. Lett. **51**, 434 (2000).

VI. Jian Huang, F. Pierre, Tero T. Heikkilä, Frank K. Wilhelm, and Norman Birge, *Observation of a controllable π-junction in a 3-terminal Josephson device*, Phys. Rev. B **66**, 020507(R) (2002).

VII. Tero T. Heikkilä, Jani Särkkä, and Frank K. Wilhelm, *Supercurrent-carrying density of states in diffusive mesoscopic Josephson weak links*, Phys. Rev. B **66**, 184513 (2002).

VIII. Jochem J. A. Baselmans, Tero T. Heikkilä, Bart J. van Wees, and Teun M. Klapwijk, *Direct observation of the transition from the conventional superconducting state to the π-state in a controllable Josephson junction*, Phys. Rev. Lett. **89**, 207002 (2002).

IX. Tero T. Heikkilä, Tommy Vänskä, and Frank K. Wilhelm, *Supercurrent-induced Peltier-like effect effect in superconductor/normal metal weak links*, HUT Report Series, TKK-F-A814 (2002) (submitted for publication).

Throughout the overview, the above mentioned papers are referred to by their Roman numerals.

Author's Contribution

The research reported in this Thesis has been carried out during the years 1998-2002 in the Materials Physics Laboratory at the Helsinki University of Technology and in the Institute for Theoretical Solid State Physics at the University of Karlsruhe, Germany. The research reported in Papers I and III was conducted in collaboration with the Condensed Matter Theory Group in the Lancaster University, UK, and in Papers VI, VII and IX with the Chair for Theoretical Condensed Matter Physics at the Ludwig-Maximilian University of Munich, Germany. The experiments for Paper IV were carried out in the Low-Temperature Laboratory at the Helsinki University of Technology, for Paper VI in the Department of Physics and Astronomy at the University of Michigan, the USA, and for Paper VIII in the Department of Applied Physics and Materials Science Center at the University of Groningen, the Netherlands.

The author has extensively contributed to the research work reported in this Thesis. In Papers I, V, VII and IX, the theoretical formulation of the problems as well as the analytical and numerical calculations were carried out by him. The author was closely involved in all parts of the work reported in Paper II, and the computer program applied in this work was partly written by him. The analytical calculations and part of the numerics for Paper III have been conducted by the author. In Papers IV, VI and VIII, partially reporting experimental work, the author had a significant role in the theoretical analysis of the observations. In addition, for Papers IV and VIII, he did most of the numerics involved in the analysis, and for Paper VI, he computed the spectral supercurrent required for the comparison between the experiments and the theory. The author has devised several computer programs and numerical algorithms used in these papers.

The author has also actively participated in reporting the research work presented in this Thesis. Papers I, III, V, VII and IX and the theoretical part of Paper IV were written by him and he has presented the work at several international conferences.

Contents

1 Introduction

An ordered medium, e.g., a crystal lattice, a ferromagnet, or a superconductor, exhibits properties, such as the solid state, magnetism or infinite conductivity, that are absent in the corresponding unordered system. The order can be described through an order parameter F which measures the degree of order and distinguishes between the ordered ($F \neq 0$) and the unordered ($F = 0$) states. In the case of a crystal lattice, the order parameter is the Fourier amplitude of the lattice vector describing the periodicity of the lattice, in ferromagnets it is the magnetization, and in superconductors the degree of the pairing of electrons. Typically, such order parameters are continuous functions in space, the variations occurring smoothly within the length scale of a coherence length. Therefore, if an unordered medium is placed in a strong contact with an ordered one, the order parameter does not abruptly change from its bulk value to zero at the contact, but leaks into the unordered material, changing its properties. Such effects are strongest in superconductors [1, 2] where at low temperatures the coherence length, being a few hundred nanometers in typical experiments, is within the reach of present-day experimental techniques. This work studies the variations in the physical systems lacking intrinsic superconductivity due to this superconducting proximity effect.

The concept of the proximity effect has been known ever since the early days of superconductivity, but its systematic study has become possible only through the development of the major branches of contemporary condensed-matter physics: nanoelectronics and mesoscopics. Residing between the macroscopic world where classical physics may be applied and the microscopic phenomena for which a complete quantum-mechanical treatment is required, mesoscopic systems allow quantum-mechanical effects such as interference to be studied in an otherwise classical circuit composed of resistors, capacitors and voltage sources. A major advance for the foundation of mesoscopic physics has been the observation that elastic scattering is not phase breaking but the phase coherence length λ_φ in normal metals is only limited by such inelastic effects as electron-phonon or electron-electron scattering. At the sub-Kelvin temperatures reached rather easily in today's experiments, the latter are small enough for the phase information of the electrons in metals to persist up to some microns. Therefore, interference effects can be observed in conductors of submicron scale. Such phase coherence is also required for the persistence of the superconducting proximity effect, being ultimately caused by interference.

The field of superconducting mesoscopics focuses on the effects of superconducting proximity on normal, non-superconducting phase-coherent material [3–5] (see Fig. 1 and micrographs of the experimental setups studied in this Thesis, Figs. 11, 14 and 17). An alternative viewpoint to the penetration of the pairing correlations is given by studying how the superconducting charge carriers, the Cooper pairs, are transmitted into the normal-metal side. At the contact between a superconductor (S) and a normal-conducting (N) material, they leak into N by creating correlated electron-hole pairs. From the point of view of the normal metal, an electron reflects from the interface in this Andreev reflection [6] as a hole and vice versa. Therefore, pair correlations on the N side depend on the interference of the electrons and holes. As a result, the conductivity of the normal

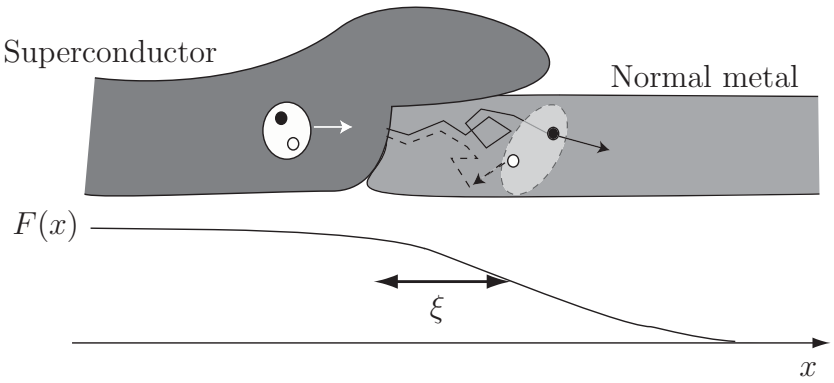

Figure 1: Typical normal-superconductor contacts for the study of the proximity effect are deposited as overlap junctions of two materials, for example superconducting aluminum or niobium and normally conducting copper or silver. As a result, Cooper pairs leak from the superconductor to the normal-metal side, creating correlated electron-hole pairs and changing the local properties of the normal metal.

metal increases [7], the local density of states is altered [8, 9], the magnetic response changes [10], and supercurrents may flow through SNS weak links [11].

In a diffusive conductor, the proximity effect persists up to length scales determined by the minimum of the phase-coherence length λ_φ and a thermal coherence length ξ_T, dependent on the diffusive motion of the electrons and holes and on their average excitation energy. Typical experiments are conducted at temperatures around and below one Kelvin, where λ_φ is of the order of microns in metals, and ξ_T hundreds of nanometers.

The interference effects in a sample of length L bring in a novel energy scale which depends on the average time spent by an electron traversing the distance L. In the diffusive case, most often encountered in metallic nanostructures, the electrons suffer multiple elastic reflections, on length scales of the order of the mean free path $l_{\rm el} \ll L$, before reaching the distance L. Thus, their motion is diffusive with the diffusion constant D and the average diffusion time is given by L^2/D. Therefore, interference effects taking place within the length scale L show a characteristic energy scale given by the inverse of this time, $\varepsilon_T = \hbar D/L^2$, usually referred to as the Thouless energy [12]. This energy scale shows up, for example, in the temperature dependence of the supercurrent, and it defines the scale separating linear and nonlinear regimes of nonequilibrium effects.

At present the equilibrium properties of metallic NS heterostructures are fairly well understood. Recently, the attention has turned into systems composed of superconductors and ferromagnets (F) [13–15]. Pairing correlations in conventional superconductors are in the spin-singlet channel, coupling electrons of opposite spins. Therefore, ferromagnets favoring only one of the spins are expected to strongly suppress the superconducting effects (see, e.g., Paper IV). However, opposite observations to this rule also exist [14, 15] and the situation has remained elusive.

The study of effects far from equilibrium is another topic which has recently received a lot of interest [7, 16, 17]. When voltages V across the mesoscopic wires in contact with superconductors exceed a few ε_T/e, the currents are no longer proportional to V, but

rather the transport coefficients start to depend on the applied voltage. Such nonequilibrium effects have also been studied within the Josephson effect [18], where supercurrents flow through N-metal weak links between two superconductors. By applying a voltage between the transverse ends of the weak link [17, 19], the maximal obtained supercurrent — the critical current of the weak link — can be tuned through the nonequilibrium. One of the remarkable consequences of this is the possibility to drive the weak link out of the conventional state to a π-state, where the direction of the supercurrent is reversed. In principle, such states could be used in quantum computing [20, 21].

Outline of the Thesis

This dissertation presents the author's work on the superconducting proximity effect in phase-coherent normal metals, presented in Papers I through IX. The overview serves to provide an introduction to these papers and is structured into three parts.

The first part, covering Secs. 2 and 3, introduces the basic phenomenology of NS heterostructures, the proximity effect and Andreev reflection, and outlines the microscopic theory developed for their description. Section 2 offers a phenomenological discussion of these effects, including a semiclassical treatment for the description of nonequilibrium effects with Andreev reflection. In Sec. 3, the microscopic theory applied in Papers I – IX is presented, and two approaches to describe proximity-affected transport properties are shown. The first of these, the scattering approach, is applied in Papers I – III, and the second one, based on quasiclassical Green's functions, in Papers IV – IX.

Examples of equilibrium and linear-response phenomena are given in Sec. 4, the second part of the overview. The basic phenomena and the theory applied to the description of heterostructures fabricated from superconductors and ferromagnets are explained in Subs. 4.1. Such systems are studied in Papers IV and V which consider the suppression of the density of states in a superconductor due to the proximity of the ferromagnet and the supercurrent through a ferromagnetic weak link, respectively. Exemplifying linear-response phenomena, Subs. 4.2 considers the effect of Andreev reflection on a normal-metal mesoscopic interference effect, the universal fluctuations of the linear conductance through a disordered metal.

The third part, Sec. 5, takes the systems studied far from equilibrium by applying a voltage V of the order of or greater than the Thouless energy. As a result of this voltage, the quasiparticle distribution functions assume complicated spatial dependence, and due to this nonequilibrium distribution, for example the supercurrent through an out-of-equilibrium SNS weak link is altered and can be tuned by variations of V. Reciprocally, the nonequilibrium distribution functions can also be controlled through the application of a supercurrent. This leads to a large out-of-equilibrium thermoelectric effect. Another example of a nonequilibrium transport phenomenon is the nonlinear behavior of the differential conductance through a diffusive NS contact. Due to the energy-dependent increased conductivity of the N wire, the conductance becomes voltage dependent [7]. In Paper II, we show that a similar voltage dependence can also be observed in the differential shot noise, which describes the time-dependent fluctuations of the current.

Section 6 summarizes our findings and discusses some open problems.

2 Phenomenology of superconducting heterostructures

In this section, basic phenomena taking place in superconductor-normal metal heterostructures are discussed. These may be described within two alternative pictures, either a picture of induced superconductivity due to the penetration of the pairing amplitude, or that of Andreev reflection. These are explained in Subs. 2.1. The previous is most often applied in the evaluation of equilibrium properties. For the description of nonequilibrium phenomena on the normal-metal side, one may take as a first approximation a semiclassical approach neglecting the proximity effect such that the only effect of superconductivity is a boundary condition given by the Andreev reflection. Such an approach, including the solutions of the electron distribution functions in a few basic cases, is given in Subs. 2.2.

2.1 Andreev reflection and proximity effect

The theory of superconductivity is based on the picture of correlated electron pairs, Cooper pairs, appearing in the conduction electron band of a metal. The quantity describing the amount of such ordering of pairs, i.e., the order parameter of the superconducting state, is called the pairing amplitude F (the rigorous definition of this quantity is given in Subs. 3.1) and it may become finite whenever the electrons share an effective attractive interaction between them[1] [1, 2]. As a result of Cooper pairing, excitation energies of non-paired single-quasiparticle states are lifted off from the Fermi energy by the superconducting gap Δ proportional to the pair potential, $\Delta = \lambda F$, the parameter λ characterizing the strength of the coupling interaction. This leads to a practical requirement for superconductivity: the temperature has to be low enough such that thermal fluctuations into these single-electron states do not cause the order parameter to vanish.

What happens if we place a superconductor (S — a metal whose state in the bulk material would exhibit a finite order parameter) in a metallic contact with a normal (N), non-superconducting metal, such that the paired electrons may "leak" from S to N? As long as the normal-state conductivities of these two metals are somewhat equal, the pairing amplitude is a smooth function across the SN boundary (in contrast to the pair potential Δ since the interaction strength λ may change abruptly across an interface between different materials). Therefore, it turns out that the correlations penetrate quite deep into N, at low temperatures hundreds of nanometers from the interface. This superconducting *proximity effect* induces superconductive properties into nearby region of the N metal, modifying its properties [7, 8, 10], and allowing for the transport of supercurrents through the N region [11].

The phenomenon can also be viewed from the normal-metal side. Consider a large normal metal connected to a large superconductor with an energy gap Δ by a metallic contact. An electron-like quasiparticle with a momentum towards the NS interface and energy below Δ cannot enter the superconductor, but due to the scattering-free interface,

[1] In conventional superconductors, such an attractive interaction is mediated by the phonons formed in the ion lattice.

it also does not suffer an ordinary reflection. As was found by Andreev in 1964 [6], something quite peculiar happens: the quasielectron is retroreflected as a quasihole, reversing all its momentum components, not just the one orthogonal to the interface. The net result of this *Andreev reflection* (AR) is an appearance of a Cooper pair in the superconductor. The opposite may also happen: a reflection of a quasihole to a quasielectron removes one Cooper pair from the superconductor. This is how the Cooper pairs "leak" into the normal metal: by creation of particle-hole pairs (see Fig. 2).

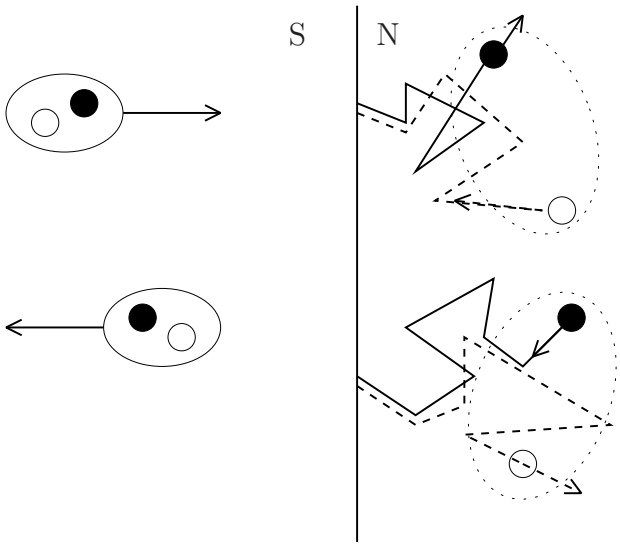

Figure 2: Proximity effect: Cooper pairs from a superconductor pop in a normal metal by creating and destroying electron-hole pairs. The superconducting correlations show up in the correlations between the wave functions for the electrons and the holes (see Subs. 3.1).

The process of Andreev reflection is essentially of two-particle form, and the effective current-carrying unit in an NS system (Cooper pair in the superconductor, an electron moving towards the interface combined with a hole moving away from it or vice versa in the normal metal) has double electron charge. Therefore, one might expect the conductance of such an NS contact to be doubled with respect to the conductance of the N wire. This is indeed observed if the normal wire is totally ballistic (free of elastic scattering), but for a more typical diffusive N wire (which shows Ohmic behavior, i.e., the resistance scales linearly with length), the conductance is essentially unchanged since also the effective path length for the quasiparticles is doubled: the Andreev reflected hole has to traverse the same distance through the wire as the initial electron. However, the doubling of effective charge can be observed also in diffusive wires, in current noise (see, e.g., [22] and Paper II), or in universal conductance fluctuations (cf. [23] and Paper I).

Another major property of AR is the reflection of energy and entropy currents: the Cooper pairs created in (or absorbed from) the superconductor do not carry energy nor entropy and therefore superconductors are very poor conductors of heat. This naturally breaks the usual coexistence of charge and thermal currents carried by the electrons and as a result, the celebrated Wiedemann-Franz or Mott laws on the behaviour of

thermoelectric transport coefficients are in general no longer valid (see Ref. [24] and Paper III).

The combination of the electron and hole may be described by a single coherent wave function, and thus they still contain the correlations carried by the Cooper pair. In other words, their correlation takes the superconducting order parameter, the pairing amplitude, to the normal-metal side. Therefore, Andreev reflection is a prerequisite for the superconducting proximity effect. The actual penetration depth for the correlations is determined by the properties of the normal metal: depending on the relative magnitude of the different effects, it is the minimum of the thermal coherence length (in diffusive structures with diffusion constant D at temperature T, it is defined as $\xi_T = \sqrt{\hbar D/\pi T}$) and the phase-coherence length λ_φ determined by the inelastic scattering processes. Hence, if the normal-metal wire is much longer than either of these lengths, one may neglect the proximity effect but, in general, not the Andreev reflection.[2]

In non-superconducting metals, macroscopic currents are formed when the distribution of quasiparticles is distorted from its typical spherical shape in the momentum space, e.g., such that there are more left- than right-moving charges. This change of the distribution function is accomplished by applying a voltage between two points, say A and B, of the structure. In this case, the established currents are dissipative: they make the increased chemical potential at A relax into the chemical potential at B. In addition to this *quasiparticle current*, the total current may also have a non-dissipative component, a *supercurrent*, in the presence of the proximity effect. This can be invoked in the normal metal if it is connected to two superconducting segments with different phases of the order parameter. As a result, current-carrying bound states appear between these segments containing an Andreev reflection at each NS contact [26, 27]. Even in the absence of a voltage at zero temperature, these states are populated and for a finite phase difference φ between the S segments, a net current can be maintained.

2.2 Semiclassical Boltzmann equation with Andreev reflection

The equilibrium phenomena in proximity-affected normal-metal structures may be described by the microscopic formalism outlined in Subs. 3.1. However, taking into account only Andreev reflection but assuming an incoherent normal-metal wire, such that the proximity effect may be neglected, allows for a rather simple study of nonequilibrium effects in the presence of superconductivity. Such an approach also serves as a starting point for the description of quasiparticle distributions in phase-coherent NS structures [28][3] ow-

[2]The characteristic length scale $\xi = \sqrt{\hbar D/E}$ for the decay of the proximity effect depends on the relevant energy scale E in a given problem. For equilibrium quantities, this energy scale is given by the temperature, but for such nonequilibrium observables as the conductance, the low-energy quasiparticles residing very near the Fermi energy have an important contribution. This leads to the "long-range coherent effects" observed in normal-superconducting systems: proximity-induced effects in the conductance decay only algebraically as a function of temperature as long as phase breaking may be neglected (see, for example, Refs. [5, 25] and Subs. 5.3).

[3]This paper takes interactions into account fully quantum-mechanically, but the superconducting effects by this phenomenological approach.

ing to the fact that phase-coherent interference effects on the diffusive-limit normal-metal distributions are typically small, second-order deviations from the incoherent case [29]. This kind of an approach has been recently utilized for example in the study of the effect of superconductivity on current noise [30, 31].

The semiclassical Boltzmann equation [32, 33] describes the average occupation number of particles $f(\mathbf{r},\mathbf{p})$ in the element $\{d\mathbf{r}, d\mathbf{p}\}$ around the point $\{\mathbf{r},\mathbf{p}\}$ in the six-dimensional position-momentum space,

$$f(\mathbf{r},\mathbf{p})\frac{\mathrm{d}\mathbf{r}\mathrm{d}\mathbf{p}}{(2\pi)^3}. \tag{1}$$

The kinetic equation for this distribution function is a continuity equation for particle flow, such that

$$\left(\frac{d}{dt} + \mathbf{v}\cdot\partial_{\mathbf{r}} + e\mathbf{E}\cdot\partial_{\mathbf{p}}\right) f(\mathbf{r},\mathbf{p};t,\varepsilon) = I_{\mathrm{el}}[f] + I_{\mathrm{in}}[f]. \tag{2}$$

Here $\mathbf{E}$ is the electric field driving the charged particles and the elastic and inelastic collision integrals I_{el} and I_{in}, functionals of f, act as source and sink terms (they illustrate the fact that scattering breaks translation symmetries in space and time — the total particle numbers expressed through the energy and momentum integrals of f still remain conserved).

In the metallic time-independent diffusive limit, Eq. (2) may be simplified as follows [34, 35]. Time independence entitles us to neglect the first term in the left-hand side, $df/dt = 0$. The electric field term can be absorbed in the space derivative by the substitution $\varepsilon \to \varepsilon - \mu(\mathbf{r})$ in the argument of the distribution function, such that ε describes the total (kinetic and potential) energy of the electron. Therefore, we are only left with the full $\mathbf{r}$-dependent derivative $\mathbf{v}\cdot\nabla f = \mathbf{v}\cdot\partial_{\mathbf{r}} f + e\mathbf{E}\cdot\partial_p f$ on the left-hand side of Eq. (2). In the diffusive regime, one may concentrate on length scales much larger than the mean free path l_{el}. There, the particles quickly lose the memory of the direction of their initial momentum (Fig. 3), and the distribution functions become nearly isotropic functions of the direction of $\mathbf{v}$. Therefore, expanding the distribution function f in the two lowest spherical harmonics in the dependence on $\hat{\mathbf{v}} \equiv \mathbf{v}/v$, $f(\hat{\mathbf{v}}) = f_0 + \hat{\mathbf{v}}\cdot\delta f$, and making the relaxation-time approximation to the elastic collision integral with the elastic scattering time τ yields the time-independent diffusion equation with a source term,

$$D\nabla^2_{\mathbf{r}} f_0(\mathbf{r};\varepsilon) = I_{\mathrm{in}}[f_0]. \tag{3}$$

Here we assume that the particles move with the Fermi velocity, i.e., $\mathbf{v} = \mathbf{v}_F$ and their diffusive motion is characterized by the diffusion constant $D = v_F^2\tau/3$.

For given boundary conditions, one may solve Eq. (3) to obtain the distribution function $f_0(\mathbf{r};\varepsilon)$. The desired dynamical observables can be evaluated from this solution, for example the charge current density is

$$\mathbf{j}_c = -eDN_0\int_{-\infty}^{\infty}\nabla_{\mathbf{r}} f_0(\mathbf{r};\varepsilon)\mathrm{d}\varepsilon \tag{4}$$

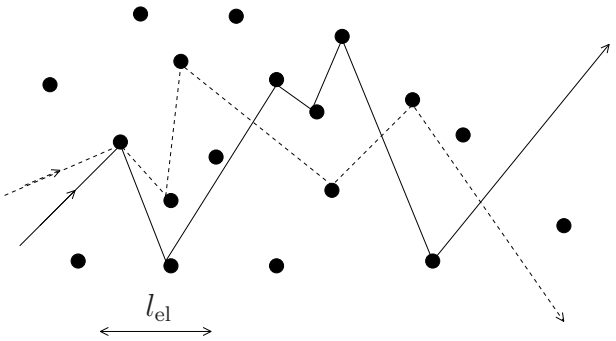

Figure 3: A particle loses its memory on its initial direction within the scale of an elastic mean free path.

and the energy current density is

$$\mathbf{j}_Q = DN_0 \int_{-\infty}^{\infty} \varepsilon \nabla_{\mathbf{r}} f_0(\mathbf{r};\varepsilon) \mathrm{d}\varepsilon. \tag{5}$$

Here N_0 denotes the density of states (including spin) at the Fermi energy, in the absence of superconductivity. Note that the charge current depends only on the even part of $f_0(\varepsilon)$ with respect to the Fermi energy, whereas the energy current depends on the odd part.

Assume a normal-metal wire connected to a large normal-metal reservoir, described via an equilibrium distribution function with temperature T and potential μ. In this case, the boundary condition to Eq. (3) at the wire-reservoir contact is given by the Fermi function $f^0 = (1 + \exp((\varepsilon - \mu)/T))^{-1}$. At an interface between the N wire and a superconducting reservoir, the Andreev reflection may be incorporated by two boundary conditions for the symmetric and antisymmetric parts of the distribution function with respect to the chemical potential μ_S of the superconductor. These are the requirements of equal electron and hole occupation numbers (the type of quasiparticles being defined with respect to μ_S),

$$f_0(\mu_S + \varepsilon) = 1 - f_0(\mu_S - \varepsilon) \tag{6}$$

and a vanishing energy current into the superconductor for energies below Δ,

$$\hat{\mathbf{n}} \cdot \nabla_{\mathbf{r}} (f_0(\mu_S - \varepsilon) - f_0(\mu_S + \varepsilon)) = 0. \tag{7}$$

Both of these conditions are given at the position of the superconducting interface. Here $\hat{\mathbf{n}}$ is the unit normal to the interface.

In multiterminal setups considered in Papers V– IX, additional boundary conditions at the crossing points of many wires are required. If the crossing points do not contain any extra scattering, these are the continuity of the distribution functions and Kirchoff-like rules for the conservation of the spectral charge and energy currents.

The above kinetic equations assume that the only current present is dissipative, due to the changes in the chemical potential. The effect of supercurrents on the distribution functions, on the level of the kinetic equations such as Eq. (3) can to some extent be taken into account by transforming to the system of co-moving coordinates where the superfluid component is at rest, i.e., where the supercurrent vanishes [33]. However, on

the level of the quasiclassical Keldysh formalism outlined in Subs. 3.3, one can accomplish this much more systematically.

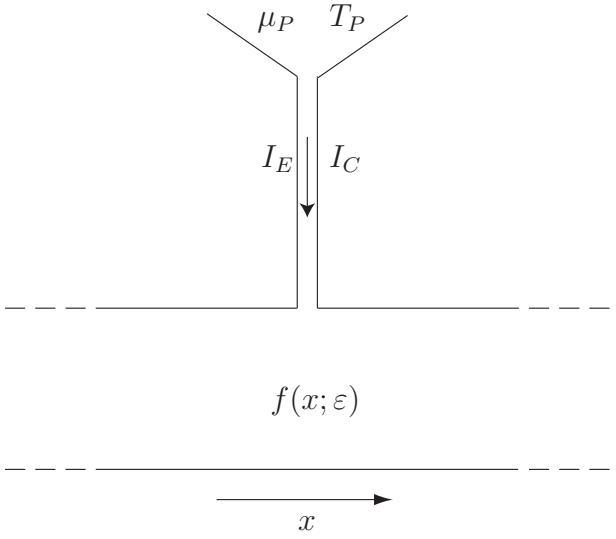

Figure 4: Schematic setup for finding the local chemical potential and effective temperature characterizing the distribution function $f(x;\varepsilon)$ of the main wire.

Effective temperature and local chemical potential

Often the space-dependent solutions to the Boltzmann equation in the diffusive limit (3) are not just Fermi functions with space-dependent temperatures and potentials. However, they may still be characterized by effective local potentials $\mu(x)$ and temperatures $T_{\rm eff}(x)$ as outlined below. The same procedure may be applied in the coherent case, including the proximity effect, described in Subs. 3.3, 5.2 and in Paper IX.

Consider a fictitious narrow normal-metal probe wire of length L, cross section A and normal-state conductivity $\sigma_N = e^2 N_0 D$ connected in position x of the main wire whose distribution function $f(x;\varepsilon)$ is characterized. From the other end, assume this probe wire to be in contact with a large reservoir with chemical potential μ_P and temperature T_P (see Fig. 4). Neglect the possible proximity effect on this wire by assuming long enough L and assume that A is much smaller than the cross section of the main wire, such that the properties of the main wire are not changed, but a current may flow in the probe wire. The electrical current in the probe wire is then

$$I_C = \frac{\sigma_N A}{eL}\int_{-\infty}^{\infty}(f(\varepsilon,x) - f^0(\varepsilon;\mu_P,T_P))\mathrm{d}\varepsilon, \tag{8}$$

and the energy current is

$$I_E = \frac{\sigma_N A}{e^2 L}\int_{-\infty}^{\infty}\varepsilon(f(\varepsilon,x) - f^0(\varepsilon;\mu_P,T_P))\mathrm{d}\varepsilon, \tag{9}$$

where $f^0(\varepsilon;\mu_P,T_P)$ is the equilibrium quasiparticle distribution function in the probe reservoir. From these two currents [32], one obtains the thermal current $I_Q = I_E - \mu I_C/e$, where μ is the local chemical potential in the probe wire.

The expressions for charge and energy currents depend on the symmetric and antisymmetric parts of the distribution function with respect to a reference energy, say μ_S. Therefore, it is convenient to separate them to even and odd parts with respect to μ_S,[4]

$$f_T(\varepsilon) = 1 - f(\mu_S - \varepsilon) - f(\mu_S + \varepsilon), \quad f_L(\varepsilon) = f(\mu_S - \varepsilon) - f(\mu_S + \varepsilon). \tag{10}$$

In the reservoirs, where the electrons are described by Fermi distribution functions, the equilibrium forms for f_L and f_T are (cf. Fig. 5)

$$f^0_{L/T} = \frac{1}{2}\left(\tanh\left(\frac{E+\mu}{2k_BT}\right) \pm \tanh\left(\frac{E-\mu}{2k_BT}\right)\right), \tag{11}$$

where μ denotes the chemical potential with respect to μ_S, and T is the temperature.

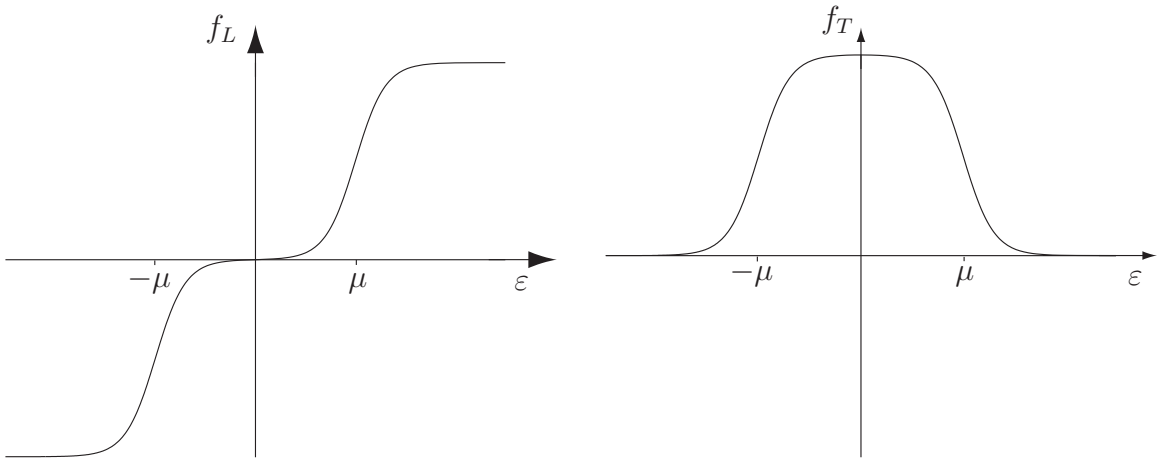

Figure 5: Equilibrium longitudinal (antisymmetric) and transverse (symmetric) distribution functions in a reservoir with a chemical potential μ.

The local chemical potential $\mu(x)$ and the effective temperature $T_{\rm eff}(x)$ are obtained by defining them such that if $\mu(x) = \mu_P$, the electrical current in the probe wire vanishes, and if $T_{\rm eff}(x) = T_P$, the heat current vanishes. Hence, we obtain the condition for the chemical potential,

$$\int_0^\infty \left(f^0_T(\varepsilon; \mu_P, T_P) - f_T(\varepsilon, x)\right) \mathrm{d}\varepsilon = 0. \tag{12}$$

The relation can be simplified further, by integrating the first part of Eq. (12) to yield

$$\mu(x) = \mu_P = \int_0^\infty f_T(\varepsilon, x)\mathrm{d}\varepsilon. \tag{13}$$

This relation shows that the symmetric function $f_T(\varepsilon, x)$ describes the local chemical potential.

The condition for the local effective temperature can be obtained analogously, by requiring

$$\int_0^\infty \varepsilon(f^0_L(\varepsilon; \mu_P, T_P) - f_L(\varepsilon, x))\mathrm{d}\varepsilon = 0. \tag{14}$$

[4]In the theory of nonequilibrium superconductivity, the subscripts L and T refer to the "longitudinal" and "transverse" changes of the superconducting order parameter, due to the two types of nonequilibrium they describe [36].

Now we can subtract from both sides of Eq. (14) the term

$$\frac{(\pi k_B T_P)^2}{6} = \int_0^\infty \varepsilon (f_L^0(\varepsilon, \mu_P, T_P) - f_L^0(\varepsilon, \mu_P, 0)) \mathrm{d}\varepsilon \tag{15}$$

to obtain

$$T_{\mathrm{eff}}(x) = T_P = \frac{\sqrt{6}}{\pi k_B} \left[\int_0^\infty \varepsilon (f_L(\varepsilon, x) - f_L^0(\varepsilon, \mu_P, T=0)) \mathrm{d}\varepsilon \right]^{1/2}. \tag{16}$$

This defines the local effective temperature as the deviation of the distribution function from the corresponding zero-temperature equilibrium function with the local chemical potential.

Distribution functions in the absence of proximity effect

The solutions to semiclassical kinetic equations cannot describe coherent phenomena due to the superconducting proximity effect, but they yield a good starting point for the exploration of these phenomena. Consider a diffusive normal wire placed between two large normal-metal reservoirs, located at $x = 0$ and $x = L$ with the chemical potentials $\mu_1 = \mu/2$ and $\mu_2 = -\mu/2$ at the temperature T, i.e., one has applied a voltage $V = \mu/e$ between the reservoirs. Moreover, assume that the inelastic scattering length is much larger than L. In this case, the quasiparticle distribution function is described by Eq. (3) with $I_{\mathrm{in}} = 0$ and with boundary conditions given by Fermi distribution functions $f^0(\varepsilon; \mu_i, T)$. The resulting space-dependent distribution function in the wire interpolates linearly between the reservoir functions,

$$f(\varepsilon; x) = \left(1 - \frac{x}{L}\right) f^0(\varepsilon; \mu_1, T) + \left(\frac{x}{L}\right) f^0(\varepsilon; \mu_2, T) \tag{17}$$

resulting in the staircase distribution function shown in Fig. 6a in the limit $\mu \gg k_B T$. The corresponding symmetric and antisymmetric parts are

$$f_T(\varepsilon; x) = \left(\frac{1}{2} - \frac{x}{L}\right) \left(\tanh\left(\frac{\varepsilon + \mu/2}{2k_B T}\right) - \tanh\left(\frac{\varepsilon - \mu/2}{2k_B T}\right) \right) \tag{18}$$

$$f_L(\varepsilon; x) = \frac{1}{2} \left(\tanh\left(\frac{\varepsilon + \mu/2}{2k_B T}\right) + \tanh\left(\frac{\varepsilon - \mu/2}{2k_B T}\right) \right). \tag{19}$$

This function was measured by Pothier *et al.* [16], showing the importance of inelastic scattering mainly due to electron-electron interactions for the shape of the distribution function in long wires (for a detailed treatment of these effects, see [37]). As a second example, replace the normal reservoir at $x = 0$ by a superconducting one, imposing the boundary conditions (6,7) at the NS interface for $\varepsilon < \Delta$. The resulting distribution function is plotted in Fig. 6b; it is given by (for simplicity, choosing now $\mu_1 = 0$ and $\mu_2 = \mu$)

$$f(\varepsilon; x) = \begin{cases} \frac{1}{2}\left(1 + \frac{x}{L}\right) f^0(\varepsilon; \mu) + \frac{1}{2}\left(1 - \frac{x}{L}\right) f^0(\varepsilon; -\mu), & |\varepsilon| < \Delta \\ \left(1 - \frac{x}{L}\right) f^0(\varepsilon; \mu = 0) + \frac{x}{L} f^0(\varepsilon; \mu), & |\varepsilon| > \Delta. \end{cases} \tag{20}$$

In this case the symmetric and antisymmetric parts are

$$f_T(\varepsilon;x) = \frac{x}{2L}\left(\tanh\left(\frac{\varepsilon+\mu}{2k_BT}\right) - \tanh\left(\frac{\varepsilon-\mu}{2k_BT}\right)\right) \tag{21}$$

$$f_L(\varepsilon;x) = \begin{cases} \frac{1}{2}\left(\tanh\left(\frac{\varepsilon+\mu}{2k_BT}\right) + \tanh\left(\frac{\varepsilon-\mu}{2k_BT}\right)\right), & \varepsilon < \Delta \\ \left(1-\frac{x}{L}\right)\tanh\left(\frac{\varepsilon}{2k_BT}\right) + \frac{x}{2L}\left(\tanh\left(\frac{\varepsilon+\mu}{2k_BT}\right) - \tanh\left(\frac{\varepsilon-\mu}{2k_BT}\right)\right). & \varepsilon > \Delta. \end{cases} \tag{22}$$

In both cases, $f_L(\varepsilon)$ is constant in space (in the NS case, for $\varepsilon < \Delta$), given by its value in the N reservoir(s), and the total electrical current is

$$I = \frac{A\sigma_N}{L}\mu/e \tag{23}$$

i.e., we obtain Ohm's law. The energy current disappears and the chemical potential interpolates linearly between those of the reservoirs. In this incoherent case, the difference between the two cases can only be observed in some other observables than the time-averaged current, such as shot noise [30].

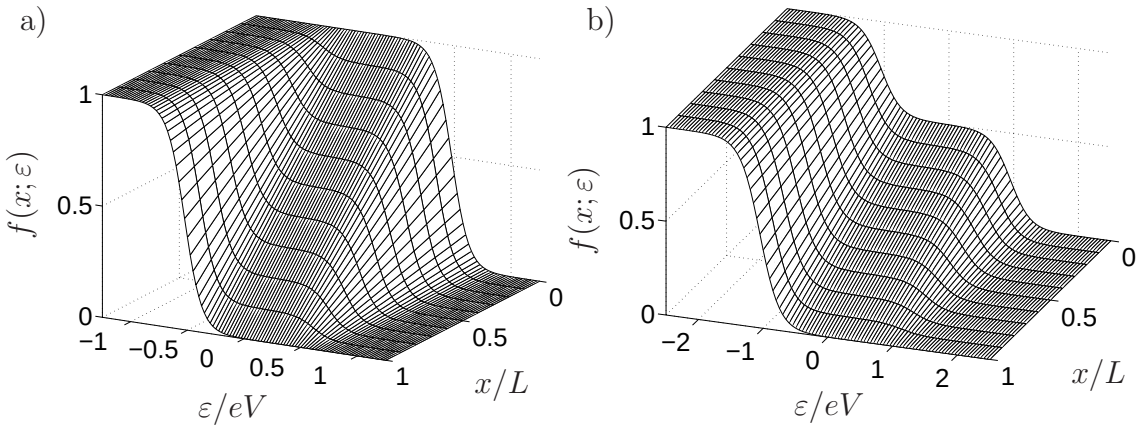

Figure 6: Nonequilibrium quasiparticle distribution function in a middle of a diffusive mesoscopic wire in the absence of inelastic scattering: a) wire placed between two normal-metal reservoirs b) wire placed between a normal-metal and a superconducting reservoir, neglecting the proximity effect. In the latter, we assume $\mu \ll \Delta$.

The local temperature characterizing the width of the region where the value of the average quasiparticle occupation number varies from unity to zero is always finite in some part of a nonequilibrium system. With a vanishing lattice temperature $T = 0$, in the N-N case

$$T_{\text{eff}} = \frac{\sqrt{3}}{\pi k_B}\sqrt{\left(\frac{eV}{2}\right)^2 - \mu(x)^2}. \tag{24}$$

Thus, since $\mu(x) = \pm eV/2$ at the reservoirs, we have there $T_{\text{eff}} = 0$, consistently with the lattice temperature. If one of the reservoirs is replaced by a superconductor, we obtain for voltages below Δ

$$T_{\text{eff}} = \frac{\sqrt{3}}{\pi k_B}\sqrt{(eV)^2 - \mu(x)^2}, \tag{25}$$

where $\mu(x)$ interpolates between the value 0 in the superconducting reservoir, and eV in the normal reservoir. Therefore, $T_{\text{eff}} = \sqrt{3}eV/\pi k_B$ near the S reservoir, indicating that since the energy current cannot flow into the superconductor, it is thermally decoupled from the mesoscopic normal-metal wire.

Above, by setting $I_{\text{in}} = 0$ we assumed the presence of only elastic scattering, due to impurities. In practice, the scattering times for electron-electron interaction [16, 37, 38] and other types of inelastic scattering such as electron-phonon or scattering due to magnetic impurities [39–41], are finite and need to be taken into account when measuring the quasiparticle distribution functions. As a general rule, these scatterings cause the local distribution function to relax towards the equilibrium type, described by the lattice temperature in the case of electron-phonon scattering and an effective temperature in the other cases. For example, they cause the function f_L to vary in space.

If one may neglect the inelastic effects, the semiclassical approach outlined above describes phase-coherent diffusive normal-metal wires with a remarkable precision, neglecting only such interference effects as weak localization. In the presence of superconductivity, the proximity effect slightly modifies the diffusion coefficients, making them space and energy dependent. A much larger variation is obtained if a supercurrent is applied through the normal-metal wire, since it couples the symmetric and antisymmetric parts of the distribution function. Subsection 3.3 indicates how the proximity-effect modifications are taken into account in the description of particle distributions, and Subs. 5.2 shows an example of a system where supercurrent can be applied to control the distribution functions.

3 Microscopic theoretical formalism

In this section, the microscopic theory of inhomogeneous superconductivity is presented and two approaches are described to quantitatively treat the transport properties of hybrid structures containing both normal and superconducting segments. The first viewpoint, taken in Subs. 3.2, is based on the approach by Landauer and Büttiker [42, 43], relating the transport properties of a mesoscopic phase-coherent sample to its transmission properties: the conductance (as well as other transport coefficients) of such a sample can be related to its scattering matrix. The second, a slightly more general approach described in Subs. 3.3, is based on the description of the local distribution function for electrons through a kinetic equation similar to the incoherent semiclassical approach, but accounting for the lowest-order phase-coherent phenomena. In both cases, for the exact calculation of the proximity-affected properties, one needs to invoke the microscopic theory of inhomogeneous superconductivity. In the previous approach, this is carried out by a direct numerical solution of the Bogoliubov-de Gennes equation [1], a Schrödinger-like equation describing the inhomogeneous superconducting structure (explained in Subs. 3.1). In the latter formalism, we may take the analytical calculations further by the quasiclassical approximation in the diffusive limit [5, 44, 45].

3.1 Andreev reflection within microscopic theory

Quasiparticle excitations in structures containing singlet superconductors with a space-dependent coupling parameter $\lambda(\mathbf{r})$ may be described with the Bogoliubov-de Gennes equation [1, 46, 47] (below, we set $\hbar = 1$)

$$\begin{pmatrix} -\frac{\nabla^2}{2m} + U(\mathbf{r}) + E_F & \Delta(\mathbf{r}) \\ \Delta^*(\mathbf{r}) & \frac{\nabla^2}{2m} - U(\mathbf{r}) - E_F \end{pmatrix} \begin{pmatrix} u(\mathbf{r}) \\ v(\mathbf{r}) \end{pmatrix} = E \begin{pmatrix} u(\mathbf{r}) \\ v(\mathbf{r}) \end{pmatrix}, \tag{26}$$

where $\Delta(\mathbf{r}) = \lambda(\mathbf{r})\langle\psi_\uparrow(\mathbf{r})\psi_\downarrow(\mathbf{r})\rangle \equiv \lambda(\mathbf{r})F(\mathbf{r})$ is the pair potential, $\lambda(\mathbf{r})$ is the local attractive interaction potential between the electrons, $\psi_\sigma(\mathbf{r})$ is the local field operator annihilating an electron at position $\mathbf{r}$ and $F(\mathbf{r})$ is the pairing amplitude. The potential $U(\mathbf{r})$ describes deviations from a regular crystal lattice, e.g., due to disorder. The pairing amplitude is obtained self-consistently from the eigensolutions of Eq. (26) via

$$F(\mathbf{r}) = \sum_n v_n^*(\mathbf{r}) u_n(\mathbf{r})(1 - 2f(E_n)), \tag{27}$$

where $f(E_n)$ is the Fermi function at the eigenenergy E_n, corresponding to the eigenfunctions $u_n(\mathbf{r}), v_n(\mathbf{r})$ of Eq. (26). It is customary to set the interaction potential $\lambda(r)$ to a finite constant in a superconductor and zero in a normal metal, since the change between the bulk values takes place within a distance of the order of the minuscule scale of a Fermi wavelength around the interface between the two materials. In the case $\Delta(\mathbf{r}) \equiv 0$, $u(\mathbf{r})$ is the wave function of an electron- and $v(\mathbf{r})$ of a hole-like excitation and hence Eq. (26) is a matrix equation in particle-hole space, often referred to as the Nambu space. For the case of a bulk superconductor, $\lambda = \text{const.}$, and one obtains the BCS energy gap Δ in the spectrum of states [1, 2, 48].

At low temperatures, the important excitations contributing to physical observables reside near the Fermi level, $\mathbf{p} \approx \mathbf{p}_F$. Therefore, we may concentrate on its neighborhood in the dispersion relation by linearizing the kinetic energy, $p^2/2m \approx \mathbf{v}_F \cdot (\mathbf{p}_F + 2\delta\mathbf{p})/2$, where $p_F \gg \delta p$. Separating the strongly oscillating part from the weakly oscillating one, we may use the Ansatz $u(\mathbf{r}) = \eta(\mathbf{r}) \exp(i\mathbf{p}_F \cdot \mathbf{r})$, $v(\mathbf{r}) = \chi(\mathbf{r}) \exp(i\mathbf{p}_F \cdot \mathbf{r})$, where $\eta(\mathbf{r})$ and $\chi(\mathbf{r})$ are slowly varying functions of the coordinate $\mathbf{r}$ (see Fig. 7). Inserting this to Eq. (26) and making the Andreev approximation [6] by neglecting the second derivatives (corresponding to quadratic terms p^2) of η, χ yields

$$\begin{pmatrix} -i\mathbf{v}_F \cdot \nabla + U(r) & \Delta(r) \\ \Delta^*(r) & i\mathbf{v}_F \cdot \nabla - U(r) \end{pmatrix} \begin{pmatrix} \eta(\mathbf{r}) \\ \chi(\mathbf{r}) \end{pmatrix} = (E - E_F) \begin{pmatrix} \eta(\mathbf{r}) \\ \chi(\mathbf{r}) \end{pmatrix}. \tag{28}$$

In what follows, we measure the energies with respect to the Fermi energy, i.e., $\varepsilon \equiv E - E_F$.

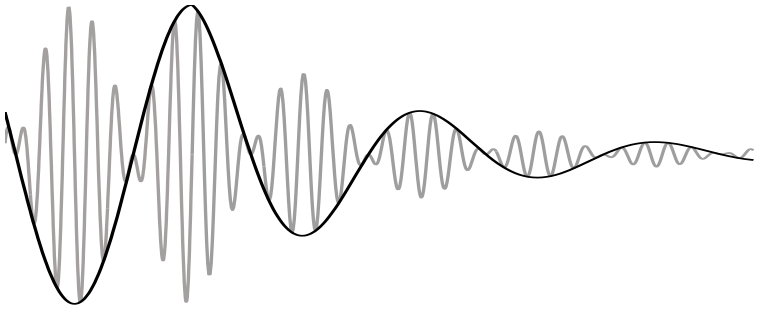

Figure 7: In the Andreev approximation, a strongly oscillating function (gray) is replaced by the product of a constant-period oscillating function and the envelope function of the oscillations (black), neglecting the second derivative of the envelope function.

As an example, consider a system of a one-dimensional clean ($U(r) = 0$) semi-infinite superconductor (located at $x > 0$) in contact with a clean semi-infinite normal metal ($x < 0$) through an insulating barrier of height U located on the interface, $x = 0$. For this example, let us assume a non-self-consistent pair potential with a step-function form, $\Delta(r) = \Delta\vartheta(x)$, where we choose $\Delta \equiv \Delta_0 \exp(i\varphi_S)$. This problem can also be solved directly from the Bogoliubov-de Gennes equation [49], Eq. (26), but let us use this as an example indicating the benefits and limitations of the Andreev approximation.

We seek for a solution of the form $\psi = \psi_{\text{left}} + \psi_{\text{right}}$ (see Fig. 8) where

$$\psi_{\text{left}} = \begin{pmatrix} 1 \\ 0 \end{pmatrix} e^{ik_N x} + r_{ee} \begin{pmatrix} 1 \\ 0 \end{pmatrix} e^{-ik_N x} + r_{he} \begin{pmatrix} 0 \\ 1 \end{pmatrix} e^{-ik_N x} \tag{29}$$

is the wave function on the left-hand side of the interface, composed of an incident electron moving towards the right, a normally reflected electron and an Andreev-reflected hole moving towards the left, each with energy ε if inelastic processes are neglected. Their wave number in the normal metal is given by $k_N \equiv \varepsilon/v_F$. On the superconducting side the electron can get transmitted into the left- and right-moving quasiparticle eigenstates,

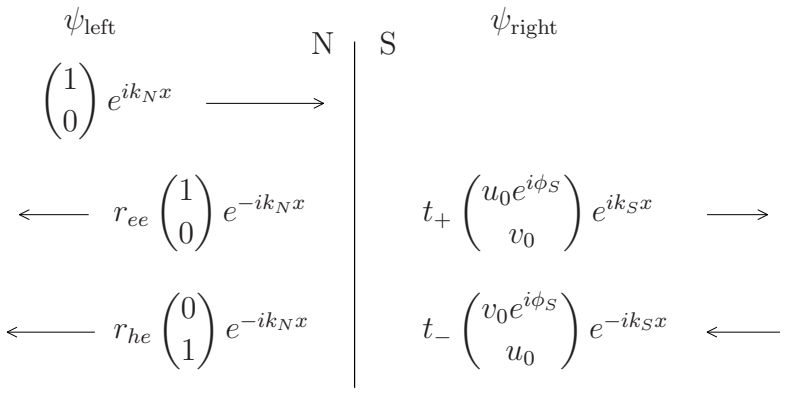

Figure 8: Andreev reflection at a NS interface.

expressed by the probabilities t_+ and t_-,

$$\psi_{\text{right}} = t_+ \begin{pmatrix} u_0 e^{i\phi_S} \\ v_0 \end{pmatrix} e^{ik_S x} + t_- \begin{pmatrix} v_0 e^{i\phi_S} \\ u_0 \end{pmatrix} e^{-ik_S x}. \tag{30}$$

The wave number in the superconductor is $k_S = \Omega/v_F$, where $\Omega = \sqrt{\varepsilon^2 - \Delta_0^2}$ and the "coherence factors" are $u_0 = \sqrt{(\varepsilon + \Omega)/2\max(\Delta_0, \varepsilon)}$, $v_0 = \sqrt{(\varepsilon - \Omega)/2\max(\Delta_0, \varepsilon)}$. We can find the transport coefficients r_{ee}, r_{he}, t_+ and t_- by matching the wave functions ψ_{left} and ψ_{right} at the interface. However, since the range of the interface potential U is assumed to be very small (in practice, it would be of the order of the Fermi wavelength λ_F), Andreev approximation is not valid near $x = 0$, and we have to resort to the Bogoliubov-de Gennes equation (26) to find the appropriate boundary conditions relating ψ_{left} and ψ_{right}. These are the continuity of the functions across the boundary, and

$$ik_F \left(\psi^L_{\text{right}}(0) - \psi^R_{\text{right}}(0) - \psi^L_{\text{left}}(0) + \psi^R_{\text{left}}(0)\right) = 2mU\psi(0), \tag{31}$$

arising from the mismatch of the derivatives of the solutions to the Bogoliubov-de Gennes equations across the boundary. Here the superscript L denotes a left-moving electron or a right-moving hole, and vice versa for R (in the superconductor, an electron branch denotes the eigensolution which tends to an electron-like wave function for large energies, $\varepsilon \gg \Delta_0$, and the hole branch is the other eigensolution).

The resulting transport coefficients are tabulated in Table I. For a vanishing interface resistance, $U \to 0$, only Andreev reflection and transmission without branch crossing (t_+) are preserved. Thus, we find that not only we have the finite probability for Andreev reflection, it is the only way to reflect from an ideal NS interface.

From the quantum-mechanical current operator, the quasiparticle charge current carried by the established state in the normal metal can for $\varepsilon < \Delta$ be found as

$$J_Q = 2ev_F|r_{\text{he}}|^2. \tag{32}$$

Hence, an Andreev-reflected electron carries twice the current compared to a normally transmitted one (ev_F), since the reflected hole carries the charge current into direction opposite to the incident electron. On the superconducting side, the quasiparticle states

	$\varepsilon < \Delta_0$	$\varepsilon > \Delta_0$
r_{he}	$\frac{e^{i\varphi_S}}{\gamma}$	$\frac{\Delta_0}{\varepsilon}\frac{e^{i\varphi_S}}{\gamma}$
r_{ee}	$\frac{-2Z(i\varepsilon + Z\Omega)}{\gamma\Delta_0}$	$\frac{-2Z(i\varepsilon + Z\Omega)}{\gamma\varepsilon}$
t_+	$\frac{\sqrt{2(\varepsilon+\Omega)}(1-iZ)e^{i\varphi_S}}{\gamma\sqrt{\Delta_0}}$	$\frac{\sqrt{2(\varepsilon+\Omega)}(1-iZ)e^{i\varphi_S}}{\gamma\sqrt{\varepsilon}}$
t_-	$i\frac{\sqrt{2(\varepsilon-\Omega)}Ze^{i\varphi_S}}{\gamma\sqrt{\Delta_0}}$	$i\frac{\sqrt{2(\varepsilon-\Omega)}Ze^{i\varphi_S}}{\gamma\sqrt{\varepsilon}}$

Table I: Wave function coefficients arising from an incident electron wave traversing towards an NS interface. Here $Z = mU/k_F$ and $\gamma = 2(u_0^2(1 + Z^2) - v_0^2Z^2)$. In the limit $Z = 0$, $\gamma = \exp(i\arccos(\varepsilon/\Delta_0))$ for $\varepsilon < \Delta_0$ and $\gamma = 1$ for $\varepsilon > \Delta_0$.

decay within the penetration depth $v_F/|\Omega|$ due to the imaginary part of k_S, and hence no quasiparticle currents are carried far from the interface. Current conservation is, however, not violated, since the quasiparticle currents are transformed into supercurrents carried by the superconducting condensate [49].

Inserting Eq. (29) into Eq. (27), with $u(x)$ the amplitude for the electron-like and $v(x)$ for the hole-like part of the total wave function, we find that the pairing amplitude F on the normal-metal side is directly proportional to the Andreev-reflection amplitude r_{he}. This holds also in the general case with an arbitrary impurity potential. Therefore, Andreev reflection generates the superconducting proximity effect, the penetration of the pairing amplitude into the normal-metal side.

3.2 Scattering approach to charge transport

In the previous subsection, an idealized example of a *scattering problem* was given and the scattering coefficients were related to the current carried through the structure. This neglected the elastic scattering due to disorder, or the momentum dependence of the scattering coefficients. These may be included by utilizing the formalism created by Landauer and Büttiker [42, 43, 50–54]. It describes a system where the sample under scrutiny divides into three different kinds of parts (see Fig. 9): The interesting region under study is the *scattering region*, where all the scattering events take place. This is connected to large incoherent particle *reservoirs* through scattering-free *leads* (labeled here by p, q). The latter define a set of basis states $|n, \alpha, p\rangle$, transverse channels, between which the scattering takes place (here, the transverse channel index is n and α denotes its type — electron or hole). Scattering is described by a scattering matrix $s^{\alpha\beta}_{np;mq}$, defined through the correlation between the "incoming" and "outgoing" basis states far off the scattering region. In the example of the previous subsection, r_{he} and r_{ee} are elements of the scattering matrix but t_+ and t_- only for $\varepsilon > \Delta$. The reservoirs are assumed

to be in equilibrium, with well-defined, reservoir-dependent chemical potential μ_p and temperature T_p and large enough such that the injected and absorbed quasiparticles do not perturb their state. The reservoirs serve to inject the electrons and holes into the transverse channels in the leads.

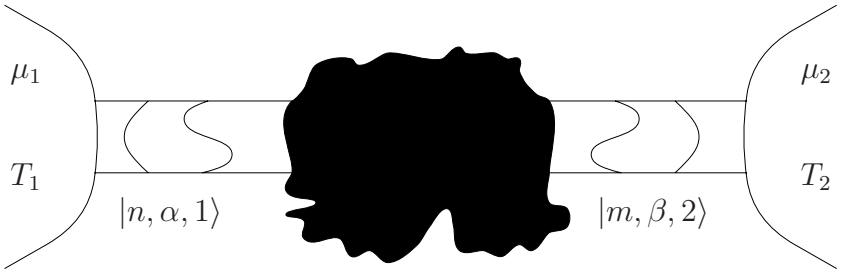

Figure 9: Two-terminal scattering geometry.

In what follows, let us consider a case where the scattering region is connected to two reservoirs, 1 and 2 (as in Fig. 9). Treating the electron- and hole-like channels separately allows one to define a matrix of scattering probabilities $P_{pq}^{\alpha\beta}$ between the electron- and hole-like states,[5]

$$P_{pq}^{\alpha\beta} \equiv \sum_{n\in p, m\in q} [s_{nm}^{\alpha\beta\,\dagger} s_{nm}^{\alpha\beta}]. \tag{33}$$

Thus, the probability for normal transmission of an electron in lead 1 to an electron in lead 2 is $T_0 = P_{21}^{ee}$ and for Andreev reflection between an electron and hole it is $R_A = P_{11}^{he}$. Within linear response (assuming that the P-matrix elements do not depend on energy on the scale of the applied voltage), one can now relate the transport coefficients of the sample to the elements of its P-matrix. For example, the conductance of a spin degenerate normal-metal wire is given by the Landauer formula,[6]

$$G_{\rm N} = \frac{e^2}{\pi} T_0 \tag{34}$$

and in the case of an NS interface [4, 55],

$$G_{\rm NS} = \frac{e^2}{\pi}(T_0 + 2R_A). \tag{35}$$

A more complicated two-probe situation can be realized by assuming a large superconductor in contact with the scattering region such that the total current into it vanishes (as in Paper I). In this case, the formula for the linear conductance between two normal reservoirs is given by [4, 56]

$$G_{\rm NSN} = \frac{e^2}{\pi}\left[T_0 + T_A + 2\left(\frac{R_A R'_A - T_A T'_A}{R_A + R'_A + T_A + T'_A}\right)\right], \tag{36}$$

where $T_A = P_{21}^{he}$ is the Andreev transmission probability from lead 1 to 2, and the primed coefficients denote probabilities from lead 2 to lead 1.

[5] This is the sum of the probabilities for different channels, and thus the elements of the P-matrix range between zero and the number of channels.

[6] In conventional units, where $\hbar$ is not chosen to unity, the prefactor is $2e^2/h$.

The conductance G is defined by the ratio between the time-averaged current and the applied voltage. However, also other types of observables can be expressed in terms of the scattering probabilities. Corresponding scattering-matrix formulae for the zero-frequency noise, describing the fluctuations of current in time, are given in [57], and applied, for example, in Paper II. Thermoelectric coefficients, e.g., the thermopower describing the voltage response to an applied temperature gradient, are related to the scattering matrix in the presence of Andreev reflection in Ref. [24]. Such a study may directly yield information on the effect of superconductivity on the relation between different response functions. For example, it is shown in Paper III that the Mott relation between the thermopower and the logarithmic energy derivative [32] of the conductance is not in general valid in the presence of Andreev reflection.

In some idealized cases, one may find the dependence of the scattering-matrix elements on the system parameters and energy analytically from rather simple considerations — as was done in the previous subsection. However, for a complicated geometry of the scattering region or in the presence of elastic scattering, one needs to resort to other methods. A widely employed approach, originally borrowed from nuclear physics, is to consider the behaviour of a whole distribution of scattering matrices, or especially of their eigenvalues — an approach referred to as random matrix theory (for a review, see [58]). Such a treatment is valid when the number of quantum channels is high as is typical especially in the scattering regions formed by metallic wires. For many systems, e.g., a diffusive normal-metal wire [59] and a dirty two-dimensional interface [60], one has indeed found an analytical formula for the distribution of transmission eigenvalues. Furthermore, at zero energy, one can relate the Andreev reflection probabilities to the transmission probabilities through the normal-metal wire [55], and thus random matrix theory yields the transport properties of NS systems under such conditions.

In many cases, the distribution of transmission eigenvalues is difficult to find analytically and one has to evaluate the scattering matrix using numerical methods. This approach has been applied in Papers I – III. In the numerics, we replace the continuum Bogoliubov-de Gennes equation (26) by its tight-binding version (for details, see Ref. [54]), where lattice sites represent sites in the crystal lattice. A typical approximation is to take into account only the nearest-neighbour couplings of strength γ. In this case, the Hamiltonian for the problem can be written in matrix form as

$$H = \sum_{\alpha=\pm1} \alpha \Big[\sum_i \varepsilon_i |i,\alpha\rangle\langle i,\alpha| + \sum_{\langle i,j\rangle} \big(\gamma |j,\alpha\rangle\langle i,\alpha| + h.c.\big) \Big] + \sum_i \big[\Delta_{ii} |i,1\rangle\langle i,-1| + h.c.\big]. \quad (37)$$

Here i, j index the lattice site, $\langle i,j\rangle$ referring to the nearest neighbours i and j, and $\alpha = \pm 1$ refers to the type of the state, $\alpha = +1$ for an electron and $\alpha = -1$ for a hole. To describe a disorder potential, the site energies ε_i may be chosen randomly from some distribution[7] of width w, such that w characterizes the amount of disorder. This model (without the last part due to the pair potential matrix Δ_{ii}) has been extensively applied, e.g., in the context of Anderson localization in disordered wires [61].

[7]For most observables, it turns out that the detailed shape of the distribution is unimportant. In Papers I – III, a uniform distribution is applied.

A given scattering region can be characterized by its dimensions (yielding the dimensions of the matrix H), disorder strength w, the phase of the nearest-neighbor coupling γ due to a magnetic field and the form of Δ_{ii}, usually assumed to be a step function. The numerical technique applied in Papers I – III finds the scattering coefficients by computing the retarded Green's function (here η is a small positive real number)

$$G^R = (E + i\eta - H)^{-1} \tag{38}$$

and relating this to the scattering coefficients between the states n, α and m, β in leads p and q through [54, 62–64]

$$s^{\beta\alpha}_{mn} = -\delta^{\beta\alpha}_{m,q;n,p} + i\sqrt{v^{\beta}_{m,q} v^{\alpha}_{n,p}}\langle m, q, \beta | G^R_{qp} | n, p, \alpha \rangle. \tag{39}$$

Finally, the desired physical observable is calculated by relating it to the scattering coefficients as in Eqs. (34–36). For a disordered system, an ensemble of observables is typically calculated for different configurations of the disorder potential — i.e., different sets of random site energies. In this way, one can describe the generic proximity-affected phenomena, for example, in the ensemble average (as in Paper II) or the standard deviation over the ensemble (as in Paper I).

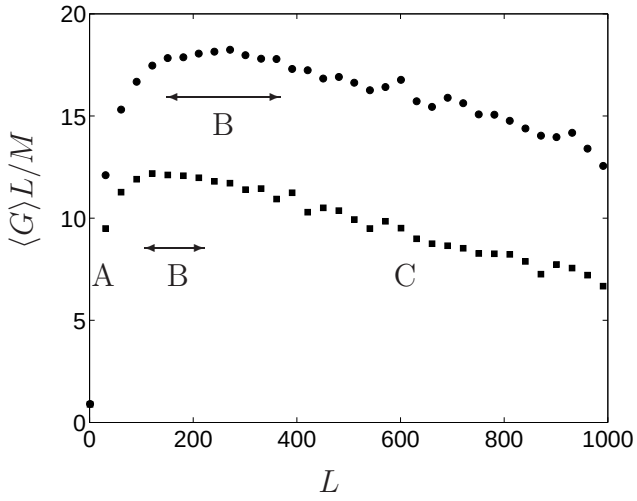

Figure 10: Mean free path can be related to the parameter w describing the disorder in the tight-binding model by observing how the quantity $\langle G \rangle L/M$ varies as the length L is varied in the system with M channels. Circles: $w = \gamma$, squares: $w = 1.25\gamma$. The regions are labeled as follows: A. Quasiballistic regime, B. Diffusive regime, and C. Localized regime. Here $M = 35$ and L is expressed in terms of the lattice constant. The scatter in the data is due to the finite number of disorder realizations.

The disorder strength w cannot be related directly to physical parameters, such as the elastic mean free path l_{el}, but the relation between the two depends on the geometry of the studied sample, especially the number of propagating channels between which the scattering occurs. Figure 10 indicates a method to relate w and l_{el} by studying how the ensemble-averaged conductance of a normal-metal wire behaves as the size of the

sample is varied. For a nearly ballistic sample, i.e., if the mean free path is very long compared to the sample size, such that most of the transmission probabilities are near to one, the conductance does not essentially depend on the length L of the sample, but only on its width M through the number of available channels for the transmission of current. In the diffusive limit $L \gg l_{\rm el}$ most relevant in our studies, the conductance is Ohmic: it scales with the cross section of the sample divided by its length. Finally, in the localized regime [65, 66] where the Anderson localization length $\lambda_{\rm loc}$ (which in the two-dimensional systems simulated in Papers I – III is always finite) is of the order of L or smaller, the conductance decreases exponentially with $L/\lambda_{\rm loc}$, but increases only linearly with the number of channels. Therefore, observing how the quantity $\langle G \rangle L/M$ behaves as a function of w and L, one can find the (quasi)ballistic, diffusive, and localized regimes for a given w.[8]

In principle, in any given NS system an observable that can be related to the scattering coefficients could be modelled by the numerical technique described above. However, the inversion of the matrix in Eq. (38) is computationally quite demanding and in order to sample enough statistics for the ensemble-averaged quantities, typically one has to compute at least a few hundred realizations. Hence, the computational time sets severe limitations on the sizes of the systems which can be studied. In practice, one is limited to two-dimensional systems with size of some hundreds of lattice sites (with the typical size of metallic crystal lattices, this would correspond to wires of size a few tens of nanometers). Therefore, for the study of phenomena not strongly dependent on the system size, one needs to take care of any finite-size effects by varying the structure size and checking how the observables respond to the variation. In the diffusive limit, the distribution of scattering matrices is universal [59], i.e., not dependent on the microscopic features of the structure. Therefore, even these small systems can be used to study generic diffusive-limit phenomena observed in wires much larger than the simulated ones.

Despite its limitations, the numerical scattering-matrix approach has some advantages over the analytical methods, e.g., those based on quasiclassical Green's functions. The latter usually consider ensemble averaged quantities, whereas the scattering-matrix approach can, in principle, describe any moment of the observable distribution, such as the universal conductance fluctuations (see Paper I). There are also some quantities in the diffusive limit for which proper analytical Green's-function theories do not yet exist, such as the proximity effect on current noise or some thermoelectric effects,[9] but which can be described within the scattering-matrix approach (see [24, 57] and Papers II and III).

[8] In the diffusive limit, weak-localization effects may, however, still be present [67, 68].

[9] For the previous quantity, a novel counting-field approach based on quasiclassical Keldysh Green's-function theory has been recently developed [69].

3.3 Quasiclassical Keldysh real-time formalism

In this subsection, the quasiclassical approach for studying inhomogeneous superconductivity is described, including nonequilibrium effects within the real-time Keldysh formalism. This formalism is applied in Papers IV – IX. Reviews of the nonequilibrium quasiclassical theory can be found in Refs. [29] and [5, 70], the latter two including the description of phenomena related to those considered in this Thesis. The fundamentals of the theory can also be read in a few recent books on superconductivity, see Refs. [71, 72]. Here we explain the main points of the formalism relevant to Papers IV – IX.

Quasiclassical approximation

In the presence of disorder or residual interactions in a Landau Fermi liquid, the most convenient method to describe the electronic properties of condensed-matter systems is through Green's functions $\hat{G}$. The treatment starts from the Gor'kov equation [73, 74], a Green's-function analogue to the Bogoliubov-de Gennes equation, but with the added benefit of the description of scattering through self-energies $\hat{\Sigma}$. In the time-independent case, it can be written in the compact form

$$\int \mathrm{d}\mathbf{r}_2(\hat{G}_0^{-1} - \hat{\Delta} - \hat{\Sigma})(\mathbf{r}_1, \mathbf{r}_2)\hat{G}(\mathbf{r}_2, \mathbf{r}_{1'}) = \delta(\mathbf{r}_1 - \mathbf{r}_{1'}). \tag{40}$$

Here $\hat{G}_0^{-1}(\mathbf{r}_1, \mathbf{r}_2) = \delta(\mathbf{r}_1 - \mathbf{r}_2)(i\varepsilon\hat{\tau}_3 + \nabla^2/2m - e\phi(\mathbf{r}_1))$ is the Green's function for an electron in a scattering-free normal metal in the potential $\phi(\mathbf{r}_1)$ and $\hat{\tau}_3$ is the third Pauli matrix in electron-hole space. The pair-potential matrix is of the form

$$\hat{\Delta} \equiv \begin{pmatrix} 0 & \Delta(\mathbf{R}) \\ \Delta^*(\mathbf{R}) & 0 \end{pmatrix}, \tag{41}$$

and the self-energy $\hat{\Sigma}$ may describe any kind of scattering, apart from that responsible for $\hat{\Delta}$.

The Gor'kov equation itself is rather difficult to solve for most inhomogeneous systems. Eilenberger [44] introduced a simplifying approximation by using the fact that the Fourier transform of $\hat{G}(\mathbf{r}, \mathbf{r}'; \varepsilon)$ with respect to the relative coordinate $\mathbf{r} - \mathbf{r}'$ is highly peaked around momenta $\mathbf{p}$ for which $|\mathbf{p}| \approx p_F$, i.e., $\hat{G}$ oscillates strongly as a function of $\mathbf{r} - \mathbf{r}'$ (the wavelength of these oscillations is thus the Fermi wavelength λ_F, typically of the order of a nanometer). In metals, these oscillations are responsible for many second-order interference effects but, for the majority of the low-order effects, the information contained in them may be ignored. Defining $\zeta \equiv p^2/2m - E_F$ and $\mathbf{R} \equiv (\mathbf{r} + \mathbf{r}')/2$ we may introduce the quasiclassical Green's function through

$$\hat{g}(\hat{\mathbf{p}}, R; \varepsilon) \equiv \frac{i}{\pi} \int \mathrm{d}\zeta \hat{G}(\zeta, \hat{\mathbf{p}}, \mathbf{R}; \varepsilon). \tag{42}$$

Now making the quasiclassical approximation of treating $\hat{G}$ as a δ-like function of $\hat{\mathbf{p}}$ yields the Eilenberger equation (for details, see Refs. [5, 70])

$$-i\mathbf{v}_F \cdot \nabla \hat{g} = \left[-i\varepsilon\hat{\tau}_3 + \hat{\Delta} + \hat{\Sigma}, \hat{g}\right]. \tag{43}$$

and $\hat{\Sigma}$ denotes the scattering self-energy. This equation preserves the square of $\hat{g}$, and using Eq. (42) in a bulk superconductor, one can show [75] that this equals $\hat{g}^2 = \underline{\hat{1}}$.

Both the quasiclassical approximation and the Andreev approximation discussed above rely on the fact that the variations in the potentials (such as disorder or structural variations) are on a scale much larger than the quasiparticle de Broglie wavelength, i.e., the Fermi wavelength. Therefore, it may not be a surprise that one can be derived from the other without additional approximations [76,77]. Both of these are essentially perturbation theories in the small parameter λ_F/ξ, the ratio between the Fermi wavelength and the coherence length $\xi = v_F/\varepsilon^*$ in the clean limit and $\xi = \sqrt{D/\varepsilon^*}$ in the diffusive case. Here ε^* is the maximum of the energy scales important for the problem, such as k_BT, Δ or eV. In other words, the theory is constructed as an expansion in ε/E_F,[10] a limit valid in the treatment of most of the phenomena related to metals and superconductors, with the exceptions of the quantum Hall effect, typical thermoelectric effects (but not all: see Subs. 5.2) and such interference effects as localization or the Aharonov-Bohm effect. The interpretation of the quasiclassical approximation is discussed in detail in Refs. [77, 78].

The Eilenberger equation, and especially its parametrization leading to Riccatti-type equations [79], are often applied to describe short-coherence-length superconductors, such as the novel high-temperature superconductors, and other structures where the elastic mean free path $l_{\rm el}$ exceeds or is of the same order as the other length scales of the problem. In these cases, Green's function is highly direction-dependent, since the information of the directions of the quasiparticles is retained up to lengths of the order of the size of the structure. However, in the diffusive limit where the elastic-scattering self-energy exceeds all the other energy scales, i.e., $l_{\rm el}$ is much smaller than the coherence length ξ and the variations in the considered structure, $\hat{g}(\hat{\mathbf{p}})$ is nearly isotropic and one may expand the dependence on the direction of $\mathbf{p}$ in spherical harmonics, retaining only the s- and p-wave parts. As a result, one arrives at an equation first derived by Usadel [45],

$$D\nabla \cdot \left(\hat{G}(R;\varepsilon)\nabla\hat{G}(R;\varepsilon)\right) = \left[-i\varepsilon\hat{\tau}_3 + \hat{\Delta} + \hat{\Sigma}_{\rm in}, \hat{G}(R;\varepsilon)\right], \tag{44}$$

where $\hat{G}(R;\varepsilon)$ is the s-wave (isotropic) part of $\hat{g}(\hat{\mathbf{p}}, R;\varepsilon)$ and $\hat{\Sigma}_{\rm in}$ describes inelastic scattering.

Real-time Keldysh approach to nonequilibrium phenomena

Equilibrium systems at a finite temperature may be described in terms of Schrödinger-type propagation in imaginary time [80], the length of the propagation being determined by the inverse temperature. As a result, it turns out that the observables are found by evaluating the Green's functions at imaginary Matsubara fermion frequencies (energies) [74, 81] $\omega_n = \pi k_B T(2n+1)$ and summing over n. However, for systems far from equilibrium (as those considered in Papers V – IX), one needs, in addition to the information of the spectral properties of the quasiparticle eigenstates in the system as in the

[10] The crucial assumption is that of the linearity of the dispersion relation around $E \approx E_F$, allowing one to write $\varepsilon(k) = \mathbf{v}_F \cdot (\mathbf{k} - \mathbf{k}_F)$. Deviations from this linearity typically occur within energies comparable to E_F.

equilibrium case, also the knowledge on the distribution of particles in the system. Such phenomena may be described within the formalism derived by Keldysh [82], essentially replacing the Green's function $\hat{G}$ in Eq. (40) by one of the form [29, 83][11]

$$\check{G} \equiv \begin{pmatrix} \hat{G}^R & \hat{G}^K \\ 0 & \hat{G}^A \end{pmatrix}. \tag{45}$$

Here $\hat{G}^R$ and $\hat{G}^A$ are the retarded and advanced Green's functions, respectively, containing information on the eigenstates of the system, and $\hat{G}^K$ is the Keldysh Green's function, which describes the occupation numbers of the different states and satisfies a Boltzmann-type kinetic equation.

Carrying out quasiclassical and diffusive-limit approximations analogously to those above, one obtains the Usadel equation for $\check{G}$, similar in form to Eq. (44), but expressed in the Keldysh $\otimes$ Nambu space, i.e., with $\hat{G}$ being replaced by $\check{G}$, the Pauli matrix $\hat{\tau}_3$ replaced by $\underline{\check{1}} \otimes \hat{\tau}_3$ and the pair potential matrix by $\underline{\check{1}} \otimes \hat{\Delta}$. The normalization condition $\check{G}^2 = \underline{\check{1}}$ yields the conditions $(\hat{G}^R)^2 = (\hat{G}^A)^2 = \underline{\hat{1}}$ and $\hat{G}^K = \hat{G}^R\hat{h} - \hat{h}\hat{G}^A$, where $\hat{h}$ is a distribution function matrix containing two real-valued free parameters. The most common choice for these parameters is to assume a diagonal $\hat{h} = f_L\underline{\hat{1}} + f_T\hat{\tau}_3$. Through the symmetry of $\check{G}$, these two functions feature the symmetries $f_L(-\varepsilon) = -f_L(\varepsilon)$ and $f_T(-\varepsilon) = f_T(\varepsilon)$ around the superconducting pair potential, chosen to define the point $\varepsilon = 0$. These can be obtained from the distribution function $f(\varepsilon)$ for electrons as in Eq. (10).

Parametrization of the distribution matrix still leaves us with two 2×2 matrices in particle-hole space, $\hat{G}^R$ and $\hat{G}^A$, each satisfying the same normalization condition. By the symmetry[12] $\hat{G}^A = -\hat{\tau}_3(\hat{G}^R)^\dagger\hat{\tau}_3$ between them, we may parametrize these functions with the two complex functions $\theta(x;\varepsilon)$ and $\chi(x;\varepsilon)$ as[13]

$$\hat{G}^R = \cosh(\theta)\hat{\tau}_3 + \sinh(\theta)\left(\cos(\chi)i\hat{\tau}_2 + \sin(\chi)i\hat{\tau}_1\right) \tag{46}$$

$$\hat{G}^A = -\cosh(\bar{\theta})\hat{\tau}_3 - \sinh(\bar{\theta})\left(\cos(\bar{\chi})i\hat{\tau}_2 + \sin(\bar{\chi})i\hat{\tau}_1\right). \tag{47}$$

The parametrization is chosen such that the function $\theta(x;\varepsilon)$ describes the degree of pairing through the magnitude of the order parameter and χ describes its phase, $F(\mathbf{R}) = \sinh(\theta(\mathbf{R}))\exp(i\chi(\mathbf{R}))$. A frequently utilized alternative, especially useful in imaginary-time calculations, is to use trigonometric functions (with the parameters $\tilde{\theta}$ and $\tilde{\chi}$, instead of the hyperbolic ones) [84]. These two parametrizations are related through $\theta = i\tilde{\theta}$, $\chi = \tilde{\chi} - i\pi/2$.

With this parametrization, neglecting inelastic scattering, the Usadel equation for the

[11] Here and below, hat $\hat{}$ and check $\check{}$ denote matrices in the Nambu and Keldysh spaces, respectively.

[12] Note that the imaginary number in the definition of the quasiclassical Green's function in Eq. (42) slightly changes the usual relations [78] between the retarded and advanced functions.

[13] Note the sign error in the definition of $\hat{G}^A$ in Refs. [5, 70].

retarded and advanced components reads[14]

$$\begin{aligned} D\nabla^2\theta &= -2i\varepsilon\sinh(\theta) + \frac{1}{2}\left(\nabla\chi\right)^2\sinh(2\theta) + i\left(\Delta\exp(-i\chi) + \Delta^*\exp(i\chi)\right)\cosh(\theta) \\ D\nabla\cdot\mathbf{j}_E &= -i\sinh(\theta)\left(\Delta\exp(-i\chi) - \Delta^*\exp(i\chi)\right), \quad \mathbf{j}_E \equiv -\sinh^2(\theta)\nabla\chi. \end{aligned} \tag{48}$$

In the absence of a supercurrent, or in the case of a superconducting reservoir to which the "inverse" proximity effect is negligible, one can approximate $\Delta = |\Delta|\exp(i\chi)$, i.e., assuming that the phase of the superconductor is independent of energy (see below for the formula for $\Delta(\mathbf{R})$). Then the last term in the first line of Eq. (48) becomes $2i|\Delta|\cosh(\theta)$ and the second line reduces to $D\nabla\cdot\mathbf{j}_E = 0$ denoting the spatial conservation of a spectral supercurrent $\mathbf{j}_E$.

The Usadel equation for the Keldysh component of the Green's function yields the kinetic equations for the two distribution functions [5, 70, 85],

$$D\nabla\cdot\mathbf{j}_L = \mathcal{L}f_T, \quad \mathbf{j}_L \equiv \mathcal{D}_L\nabla f_L - \mathcal{T}\nabla f_T + j_S f_T \tag{49}$$

$$D\nabla\cdot\mathbf{j}_T = \mathcal{R}f_T, \quad \mathbf{j}_T \equiv \mathcal{D}_T\nabla f_T + \mathcal{T}\nabla f_L + j_S f_L, \tag{50}$$

where the kinetic coefficients depend on the solutions to the retarded and advanced parts of the Usadel equation and are given in Table II. For example, the source/sink terms $\mathcal{L}$ and $\mathcal{R}$ are nonzero only in a superconductor where $\Delta(x) \neq 0$.

$\mathcal{D}_L$	$\frac{1}{4}\mathrm{Tr}[1 - \hat{G}^R\hat{G}^A]$	$\frac{1}{2}[1 + \cosh(\theta)\cosh(\bar{\theta}) - \sinh(\theta)\sinh(\bar{\theta})\cos(2\mathrm{Im}\chi)]$
$\mathcal{D}_T$	$\frac{1}{4}\mathrm{Tr}[1 - \hat{G}^R\hat{\tau}_3\hat{G}^A\hat{\tau}_3]$	$\frac{1}{2}[1 + \cosh(\theta)\cosh(\bar{\theta}) + \sinh(\theta)\sinh(\bar{\theta})\cos(2\mathrm{Im}\chi)]$
j_S	$\frac{1}{4}\mathrm{Tr}[\hat{\tau}_3(\hat{G}^R\nabla\hat{G}^R - \hat{G}^A\nabla\hat{G}^A)]$	$\mathrm{Im}\{-\sinh^2(\theta)\nabla\chi\} \equiv \mathrm{Im}\{j_E\}$
$\mathcal{T}$	$\frac{1}{4}\mathrm{Tr}[\hat{G}^A\hat{G}^R\hat{\tau}_3]$	$-\frac{1}{2}\sinh(\theta)\sinh(\bar{\theta})\sinh(2\mathrm{Im}\chi)$
$\mathcal{L}$	$\frac{1}{2}\mathrm{Tr}[\hat{\tau}_3\hat{\Delta}(\hat{G^A} - \hat{G^R})]$	$-i\mathrm{Im}(\Delta e^{i\mathrm{Re}\chi}(\sinh(\theta)e^{-\mathrm{Im}\chi} + \sinh(\bar{\theta})e^{\mathrm{Im}\chi}))$
$\mathcal{R}$	$\frac{1}{2}\mathrm{Tr}[\hat{\Delta}(\hat{G^R} + \hat{G^A})]$	$\mathrm{Im}(\Delta e^{i\mathrm{Re}\chi}(\sinh(\theta)e^{-\mathrm{Im}\chi} - \sinh(\bar{\theta})e^{\mathrm{Im}\chi}))$

Table II: Kinetic coefficients in terms of retarded and advanced Green's functions and in the $\{\theta, \chi\}$-parametrized form. The trace goes over the particle-hole Nambu space. For a real-valued phase χ, $\mathcal{T} = 0$ and $\mathcal{L} \neq 0$ only for $\varepsilon > \Delta$.

In the absence of the supercurrent, $\nabla\chi = \mathrm{Im}\chi = 0$, thus $j_S = \mathcal{T} = 0$ and the two kinetic equations are decoupled, describing independently the behavior of the two distribution functions. In the limit of a vanishing proximity effect in a normal metal

[14] Additionally, this parametrization requires a gauge transformation from Δ to $\Delta e^{i\pi/2}$ compared to Eq. (41).

far away from the NS interface, $\mathcal{D}_L \to 1$, $\mathcal{D}_T \to 1$, we obtain the semiclassical kinetic equation (3) with $I_{\rm in}[f] = 0$.

In particle or heat reservoirs, the boundary conditions for the kinetic equations are given by the local equilibrium forms of Eq. (11). However, for $\varepsilon < \Delta$, we have $\mathcal{D}_L = 0$ in a superconductor. Therefore, since also $\mathcal{T} = 0$ and $f_T = 0$ in a superconductor in the absence of a charge imbalance [2], we find that j_L vanishes identically and thus superconductors prohibit energy transfer for sub-gap energies. As a result, near an interface between a narrow normal-metal wire and a superconducting reservoir, we obtain the boundary conditions

$$\begin{aligned} f_T(\varepsilon) &= 0 \\ \hat{\mathbf{n}} \cdot \nabla f_L(\varepsilon < \Delta) = 0, \quad f_L(\varepsilon > \Delta) &= \tanh\left(\frac{\varepsilon}{2k_B T}\right) \end{aligned} \tag{51}$$

where $\hat{\mathbf{n}}$ is chosen perpendicular to the SN interface. These are the same conditions as Eqs. (6–7) in the phenomenological theory.

If the inverse proximity effect into the superconductor becomes important (as is the case considered in Paper IV), we need to calculate $\Delta(\mathbf{R})$ self-consistently from

$$\Delta = \frac{\lambda N_0}{4i} \int_{-\infty}^{\infty} \mathrm{d}\varepsilon f_L(\varepsilon)(F^R - F^A) = \frac{\lambda N_0}{2i} \int_{-\infty}^{\infty} \mathrm{d}\varepsilon f_L(\varepsilon) \mathrm{Re}\left\{\sinh(\theta) e^{i\chi}\right\}. \tag{52}$$

At equilibrium (studied, e.g., in Paper IV), $f_L(\varepsilon)$ reduces to $\tanh(\varepsilon/(2k_BT))$ in which case one may calculate the integral by summing over the poles of f_L, corresponding to the fermionic Matsubara frequencies ω_n.

Observables

Perhaps the most usual "observable" discussed in the theory of inhomogeneous superconductivity is the local density of quasiparticle states $N(x;\varepsilon)$. This can be directly evaluated from the retarded part of the Keldysh Green's function through

$$N(x;\varepsilon) = \frac{N_0}{2} \mathrm{Re}\left\{\mathrm{Tr}\left[\hat{\tau}_3 \hat{G}^R(x;\varepsilon)\right]\right\} = N_0 \mathrm{Re}\left\{\cosh(\theta(x;\varepsilon)\right\}, \tag{53}$$

Here, N_0 denotes the density of states in the absence of superconductivity. Although not directly measurable, the local density of states can be extracted from a tunnelling current (see, for example, Refs. [2, 9] and Paper IV).

In a normal metal with $\Delta = 0$, the conserved quantities $\mathbf{j}_T$ and $\mathbf{j}_L$ denote spectral charge and energy current densities, respectively, and the corresponding observable current densities are

$$\mathbf{j}_c = \frac{\sigma_N}{2e} \int_{-\infty}^{\infty} \mathrm{d}\varepsilon \mathbf{j}_T = \frac{\sigma_N}{2e} \left[\int_{-\infty}^{\infty} \mathrm{d}\varepsilon (\mathcal{D}_T \nabla f_T + \mathcal{T} \nabla f_L) + \int_{-\infty}^{\infty} \mathrm{d}\varepsilon j_S f_L\right] \tag{54}$$

$$\mathbf{j}_Q = -\frac{\sigma_N}{2e^2} \int_{-\infty}^{\infty} \mathrm{d}\varepsilon\varepsilon \mathbf{j}_L = -\frac{\sigma_N}{2e^2} \left[\int_{-\infty}^{\infty} \mathrm{d}\varepsilon\varepsilon (\mathcal{D}_L \nabla f_L - \mathcal{T} \nabla f_T) + \int_{-\infty}^{\infty} \mathrm{d}\varepsilon\varepsilon j_S f_T\right]. \tag{55}$$

Both consist of a dissipative part (which vanishes if the distribution functions do not vary in space) and a supercurrent part (for both currents, vanishes for space independent phase χ and in the case of j_Q, also in equilibrium). Here $\sigma_N = e^2 N_0 D$ is the normal-state conductivity of the metal.

Boundary conditions for quasiclassical Green's functions: combination of scattering and quasiclassical theories

Designed to describe coarse-grained properties of superconducting heterostructures at length scales much larger than the Fermi wavelength (and for the Usadel equation, longer than the elastic mean free path), the quasiclassical theory cannot treat variations within these small length scales. A typical large variation over a short distance is an interface between different types of materials, containing some extra scattering either due to an oxide layer formed on the interface, or due to a mismatch between the normal-state conductivities of the two materials. In this case, the quasiclassical Green's functions on both sides of the interface have to be related by a boundary condition. An example of such a boundary condition for the case of Andreev-approximated wave functions was given in Subs. 3.1. For the Eilenberger functions, the boundary condition was first derived by Zaitsev [86], and this condition was later simplified in the diffusive limit by Kuprianov and Lukichev for a tunnelling interface [87]. A major invention was due to Nazarov [88], who treated the boundary condition as a form of current conservation through the interface. In the diffusive limit, a general relation between the Green's function $\check{G}_1$ on the left-hand side of the interface and $\check{G}_2$ on the right-hand side was obtained, given through the transmission eigenvalues T_n of the interface,

$$\sigma_N^1 A_1 \check{G}_1 \partial_x \check{G}_1 = \sigma_N^2 A_2 \check{G}_2 \partial_x \check{G}_2 = \frac{2e^2}{\pi} \sum_n \frac{T_n[\check{G}_1, \check{G}_2]}{4 + T_n(\{\check{G}_1, \check{G}_2\} - 2)}, \tag{56}$$

where both interfaces are assumed perpendicular to the x-direction and A_i denote the cross sections and σ_N^i the normal-state conductivities of the two wires ($i \in 1, 2$). This boundary condition relates the matrix currents $\sigma_N^i A_i \check{G}_i \partial_x \check{G}_i$ to another matrix current flowing across the interface. This equation is valid for any kind of an interface, as long as its transmission eigenvalues are known. Thus, to fully account for the effects an interface has on the quasiclassical Green's functions, we need to apply scattering theory.

In most cases, it is impossible to know the individual transmission eigenvalues of a given interface. However, applying random matrix theory [58], one may find the distribution of the eigenvalues for a given type of an interface. And since such interfaces typically contain thousands of scattering channels, one may transform the sum in Eq. (56) to an integral over the transmission eigenvalues, weighted by their distribution function (for example, see Eqs. (8–11) in Paper VII and Eqs. (3-5) in Paper V).

With Eq. (56), one may also find the boundary condition in the case of a reservoir, i.e., when its area A_2 is much larger than the area A_1 of the wire connecting to it. In the limiting case $A_2/A_1 \to \infty$ we obtain $\check{G}_2 \partial_x \check{G}_2 \to 0$, and therefore, $\check{G}_2$ is given by equating the rhs. of Eq. (44) to zero. In a superconductor with phase ϕ we then obtain $\theta_2 = \operatorname{artanh}(|\Delta|/\varepsilon)$, $\chi_2 = \phi$ whereas in a normal metal, $\theta_2 = 0$ and χ_2 is arbitrary.

Quasiclassical Keldysh and scattering-matrix approaches are powerful tools to treat most of the transport phenomena taking place in NS heterostructures and they have been applied to describe numerous phenomena. The following two sections show a few examples of these, the first concentrating on equilibrium and linear-response effects and the second one on systems far from equilibrium.

4 Equilibrium and linear-response phenomena

This section considers two examples of equilibrium and linear-response properties of superconductor-normal metal heterostructures. In equilibrium, the electron distribution function is given by the Fermi function and it does not have to be separately evaluated from a kinetic equation. In this case, the most natural observables in superconductor-normal metal heterostructures are the space-dependent density of states (DOS), varying between the bulk superconducting DOS [1, 2] and the essentially constant normal-metal DOS, and the supercurrent through a normal-metal weak link. Such equilibrium effects are described in the context of superconductor-ferromagnet heterostructures in Subs. 4.1 and in Papers IV and V.

A linear-response situation where currents can flow is obtained when such a small voltage is applied that the distribution functions vary at most linearly between two equilibrium functions with slightly different chemical potentials μ_1 and μ_2. In the framework of the scattering-matrix approach, this corresponds to the case when the elements of the P-matrix do not depend on the energy within the window between μ_1 and μ_2. In this case, the equilibrium properties of the system determine the current obtained. An example of a linear-response phenomenon which can be rather easily treated with the numerical scattering-matrix approach but which is difficult to describe analytically with the Keldysh Green's-function methods is the description of universal conductance fluctuations (UCF) in systems composed of normal and superconducting elements. In mesoscopic systems smaller than or of the order of the phase coherence length, UCF show up as a seemingly random but reproducible variation of the linear conductance as a function of magnetic field or Fermi energy. Remarkably, the magnitude of these fluctuations, described by the variance of the conductance values, has a universal value, of the order of the quantum of conductance e^2/h. This value depends on the symmetry of the system studied [89, 90], but only weakly on its shape or the overall conductance. In Subs. 4.2 and in Paper I, we discuss how Andreev reflection modifies the conductance fluctuations.

4.1 Superconductor-ferromagnet heterostructures

Superconductors (S) and ferromagnets (F) are both ordered materials, but with quite different types of the order parameter. Whereas the ferromagnetic ordering expressed through the magnetization tends to favor aligned spins of the conduction electrons, the order parameter of a conventional superconductor is in the spin-singlet channel. Therefore, in most cases ferromagnetic and superconducting order parameters tend to exclude each other. One of the reasons for the difficulty of finding coexistent superconductivity and ferromagnetism is also the different energy scales usually encountered in these two phenomena. The conventional superconducting energy scales are typically at most some 10 K (for example, the critical temperature for bulk Nb is 9.3 K), still on the scale where the deviations in the dispersion relation of electrons in the conduction band need not be taken into account. In contrast, itinerant ferromagnets rely on these variations especially through the variation of the density of states and, partially therefore, their critical temperatures are much higher (the Curie temperatures of conventional ferromagnets Fe, Co

and Ni are hundreds of Kelvin).

Concentrating on the "superconducting" temperature scales, the theory of SF heterostructures may usually assume ferromagnetism itself be unaffected by the proximity of other materials, or variations in quantities such like temperature or voltage.[15] In this case, the ferromagnets may be described by the Stoner model [93] with a constant exchange field $2h$ separating the two spin bands. Here, we assume that superconductivity and ferromagnetism are encountered in different materials, i.e., every time $\Delta \neq 0$, we must have $h = 0$ and vice versa. For the case of the interplay of ferromagnetism and superconductivity, see for example Refs. [94, 95].

Compared to the usual picture of inhomogeneous superconductivity, the description of ferromagnetism makes two additions to the theory. First of these is a new additional field, exchange field h, entering the equations as a $\hat{\tau}_3 \otimes \hat{\sigma}_3$-term in the Nambu $\otimes$ spin space, similar to the Zeeman splitting. The second new feature is the spin polarization: since the Fermi levels for the two spins are different (separated by the h), also all the effective quantities, such as the effective mass, the Fermi velocity, the density of states at the Fermi level, may be spin dependent. On the large energy scales where one takes into account the full information of the electronic band structure, exchange field and the spin-dependent Fermi velocities are necessarily related. However, for low-temperature theories involving superconductivity, one may neglect the large-scale band-structure effects, and treat these two quantities independently.

The effect of spin polarization on superconductivity has been treated within the scattering approach [96]. The clearest new phenomenon is the reduction of the Andreev reflection probability due to the spin-dependent densities of states in the ferromagnet (see [97, 98] and the references therein). Conversely, the aim is to use Andreev reflection to measure the spin polarization at the Fermi level to compare with electronic structure calculations. Below, we concentrate on the unpolarized case neglecting the effects of spin dependence of the Fermi velocities, and studying the effect of the exchange field. Assuming that the magnetic length v_F/h is much larger than the mean free path, one arrives at a modified Usadel equation [99] with the term $h\hat{\tau}_3 \otimes \hat{\sigma}_3$ (the opposite regime is treated, for example, in Refs. [100, 101]). This is similar to a strong Zeeman-splitting term due to a magnetic field and thus, an analogous situation would be observed in a very thin layer of normal material, under a strong magnetic field parallel to the normal layer (such that the orbital effects of the magnetic field may be neglected). The main effect of this field is to suppress the proximity effect into a ferromagnet and introduce a new decay scale $\xi_m = \sqrt{D/h}$ in the problem, along with oscillations of the order parameter on the same scale [102, 103]. Since in a typical ferromagnet, such as Co, Ni, or Fe, ξ_m is at most of the order of few nanometers, one expects that the proximity effect should not be observed at all over typical experimental length scales of a few hundred nanometers.

Observations by Giroud *et al.* [14] and Petrashov *et al.* [15, 104] indicate a contrary

[15] There are, of course, a few exceptions to this rule: If the ferromagnets are extremely thin, of the order of a few nanometers [91], or if one considers the effects of applied fields or temperature to the domain structure in the ferromagnet. Furthermore, a large superconductor may make inhomogeneous magnetic ordering near the SF interface more favourable than in the bulk of the ferromagnet [92].

behavior to the predicted short-scale decay of the pairing amplitude: a long-range effect of a superconductor in the conductance through a strong ferromagnet (Co and Ni, respectively). Some of these observations can be explained by the changes in the superconductor-ferromagnet interface resistance when the temperature is decreased below the superconducting transition temperature [105], but this cannot explain all of the experimental results [106, 107]. Nevertheless, there also exist opposite observations supporting the theory of a short-scale decay [108].

One of the possible explanations for the existence of the long-range proximity effect into ferromagnets is given by a formation of a triplet pairing amplitude, containing terms of type $\langle\psi_\sigma\psi_\sigma\rangle$, at the SF contact due to magnetic interface scattering [100, 109, 110] — as opposed to the usual singlet amplitude $\langle\psi_\sigma\psi_{-\sigma}\rangle$, the triplet pairing amplitude contains a term diagonal in the spin space. This does not couple to the $\hat{\tau}_3 \otimes \hat{\sigma}_3$ term given by the exchange field, and can hence penetrate to large distances, similar to the usual proximity effect into a nonmagnetic metal. In a bulk of a singlet superconductor, such a triplet part does not exist, but the magnetic scattering from possible magnetic inhomogeneities at the interface between a superconductor and a ferromagnet may give rise to a finite triplet pairing amplitude. Another alternative solution to the problem is the long-range persistence of correlations between electrons and holes upon a "crossed" Andreev reflection near a domain boundary [111]. Until some more insight on the nature of magnetic interface scattering or on the domain-structure effects is obtained, the long-range proximity effect cannot be considered totally explained.

Ferromagnetic proximity effect on superconductors

Since the singlet proximity effect is expected to be subdued in a ferromagnet during a very short interval, this should also be seen in the superconducting side near the boundary. As the pairing amplitude $F(x)$ through an ideal interface between wires of equal cross section is a smooth function, the boundary condition at a SF interface is a nearly vanishing electron-hole correlation. The changes of $F(x)$ in a superconductor take place typically within the scales of the coherence length ξ_0 (in the diffusive case, $\xi_0 = \sqrt{\hbar D/2\Delta}$), and thus the suppression of $F(x)$, and hence for example of the gap in the local density of states, may be expected to persist up to at least a few ξ_0. This inverse proximity effect was measured in Paper IV (see Fig. 11), showing a very good agreement with the predictions of the quasiclassical theory. In these calculations, the proximity effect on the ferromagnetic Ni was assumed to be completely suppressed. The only fitting parameter in the theory was the resistance of the interface at a temperature above the critical temperature of the superconducting Al. The order of magnitude of this resistance could be estimated from the measurements, and it was taken into account through the Nazarov boundary condition for a dirty interface, explained in Subs. 3.3.

In addition to the inverse proximity effect due to the boundary condition given by the rapid decay of the pairing amplitude into the ferromagnet, there may in principle exist also other types of effects of the ferromagnetic proximity on the superconductor. These are the penetration of spin polarization into the superconducting side (i.e., a ferromagnetic proximity effect [103, 112, 113]), and the magnetic field due to the spins aligned

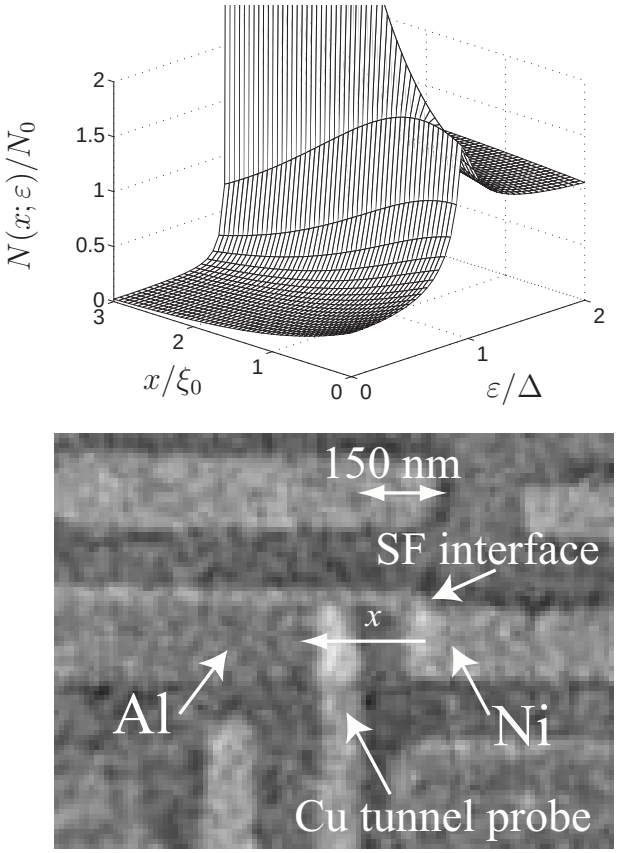

Figure 11: Top: local density of states in the superconducting side of the SF heterostructure. At $\varepsilon = \Delta$, $N(x;\varepsilon)$ quickly increases, reflecting the BCS divergence in a bulk sample. This has been cut around $N(x;\varepsilon) \approx 2$ for clarity. Bottom: closeup of the SF structure from experiments described in Paper IV (courtesy of M. Sillanpää, texts and arrows added by the author). There, the superconducting coherence length $\xi_0 = 150$ nm.

in the ferromagnet. However, the excellent agreement between the experiments and the simplified theory presented in Paper IV, and the weak response of the system to an external applied magnetic field, show that on the scale of the superconducting coherence length, both of these effects may be neglected.

SFS supercurrent

One of the important effects of the exchange field on the usual superconducting properties is the oscillation of the critical current through a ferromagnetic weak link as a function of the width d of the weak link, superimposed on the exponential overall decay (see Refs. [102, 114] and Paper V). Negative values of the critical current correspond to the π-state where the supercurrent has a different sign and the ground state of the system corresponds to a phase difference π between the superconducting contacts [115].

The oscillation in the supercurrent has been measured in a weak ferromagnet, an alloy of Cu/Ni with a Curie temperature of the order of 20 K [116,117]. In these experiments,

one cannot directly vary the exchange field, but the detailed theory of this phenomenon (see Paper V) indicates that the exchange field required for the transition from the conventional supercurrent state to the π-state depends on temperature and hence, by varying the temperature, one can observe the very sharp behavior of the critical current, including a cusp at the transition point.

The h-dependent Josephson supercurrent is formally analogous to a nonequilibrium-controlled supercurrent, as shown in Paper V. This analogy along with a method to combine both effects from (weak) ferromagnetism and nonequilibrium are explained in detail in the following section.

Research on superconductor-ferromagnet heterostructures spans a broad range of phenomena, of which many are important for large-scale applications (for example, the effect of superconductivity on giant magnetoresistance used in memory elements has been recently studied using the concepts outlined above [118]). The theoretical description of these phenomena still contains many open problems, some of which are mentioned above. Therefore, more research, both theoretical and experimental, is required for a detailed understanding of the physics of SF structures.

4.2 Universal conductance fluctuations

One of the genuine mesoscopic effects taking place in phase-coherent wires is the fact that the conductance of a disordered sample with size smaller than the phase coherence length is not necessarily self-averaging [90]. Even if the wire is much larger than the correlation length of disorder, i.e., the mean free path, its conductance does not tend to the value averaged over the configurations of disorder. Rather, an ensemble of such conductors shows a large variation of conductances, of the order of the squared conductance quantum[16] $(e^2/h)^2$ (for an example, see Fig. 12). A similar, seemingly random but reproducible variation can be observed in the conductance of such a wire by varying the magnetic field [119] or the Fermi energy by tuning a gate voltage [120]. The magnitude of these fluctuations has been shown to be universal [121–123], i.e., not to depend on the actual average value of the conductance.

The origin of the conductance fluctuations lies in the quantum interference of the different electron paths contributing to the current in the diffusive limit. If the inelastic effects are weak on the scale of the size of the conductor, the phase memory of the electrons is retained within these paths and, therefore, the interference pattern persists. For example, displacing a single impurity in a two-dimensional conductor by a distance of the order of the Fermi wavelength is sufficient to change the conductance of the whole sample by an amount of the order of $e^2/(hn_i^2 l)$ (where n_i is the impurity concentration), independent of the size of the system.

The magnitude of the UCF in normal systems can be evaluated analytically through diagrammatic methods [89,121–123] or through the random matrix theory [124–127], the latter based on the Landauer conductance formula. Both of these yield for the variance of conductances — in a quasi-1D system where the transverse directions are much smaller

[16] For clarity, in this discussion we return back to the conventional units where $\hbar \neq 1$

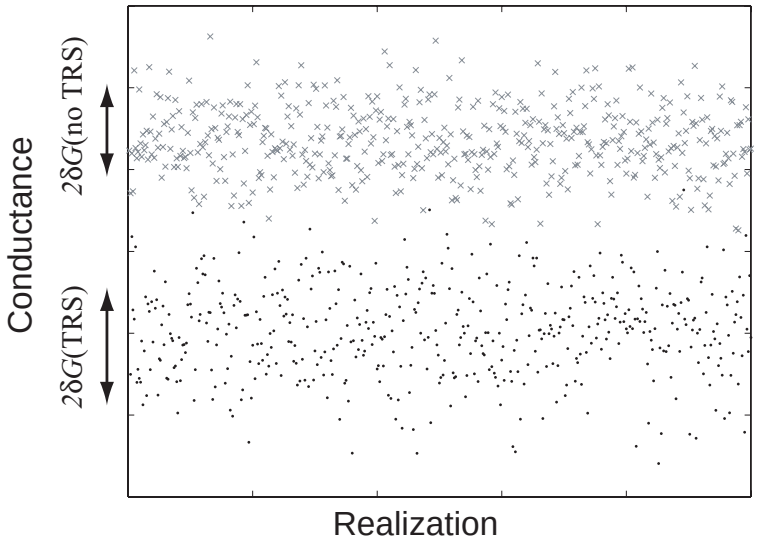

Figure 12: Universal conductance fluctuations: conductances for different realizations of disorder in conductors sharing the same dimensions and mean free path fluctuate by an amount mostly dependent on symmetry. Black dots represent an ensemble of conductances in the absence and grey crosses in the presence of the magnetic field in an "open" interferometer of Paper I. The latter have been shifted upwards for clarity.

than the longitudinal one — the universal numbers,

$$\mathrm{Var}G = \frac{8}{15\beta}\frac{e^2}{h}. \tag{57}$$

Here the parameter β depends on the symmetry [58] and it is $\beta = 1$ in the presence of a time-reversal (TRS) and spin rotation (SRS) symmetry, $\beta = 2$ in the absence of TRS and $\beta = 4$ in the absence of SRS.

These theories also yield the correlation energy and field for the fluctuations. Varying the Fermi energy, the correlations between conductances persist to variations of the order of the Thouless energy $\varepsilon_T = \hbar D/L^2$, depending on the diffusion constant D and length L of the mesoscopic wire, and the characteristic magnetic field with which the conductance fluctuates is of the order of the field producing a flux quantum $\phi_0 = h/e$ through the wire.

Besides the purely normal system, the conductance fluctuations in an NS contact in the presence of Andreev reflection can also be described analytically, especially within the random matrix theory [127]. For example, for an ideal contact, one finds that the linear conductance at $T = 0$ is essentially unchanged compared to its value without the superconductor, whereas the magnitude of UCF is greatly enhanced. The values of Var$G$ for the different symmetries are detailed in [128] and in Paper I.

In contrast to RMT, a diagrammatic approach to fluctuations in the presence of Andreev reflection becomes difficult. Therefore, Ref. [129] made a simplifying assumption that the average phase shift incurred during Andreev reflection vanishes, and could thereby calculate the magnitude of the fluctuations of a NS system. However, the value

that was obtained in the presence of TRS differs from the prediction of the random matrix theory [128]. In Paper I, we studied the conductance fluctuations in an Andreev interferometer where the phase difference between two superconducting segments can be varied, and showed that this difference is indeed due to the phase-shift assumption.

A numerical study of the fluctuations based on the scattering-matrix approach in normal-metal systems and in NS contacts has been conducted in Refs. [130] and [67], respectively. These papers, as also Paper I, study fluctuations by computing the conductances through a diffusive wire with different configurations of disorder. In contrast to Refs. [67, 130], which discuss two-terminal systems, a multiterminal situation composed of a normal wire in contact to one or more superconducting segments is considered in Paper I. No quasiparticle current is assumed to flow into the superconductors, and thus the fluctuations remain universal. Such a setup allows one to tune the phase difference between the two superconductors, for example by varying a magnetic field or driving a supercurrent between them.

The effect of Andreev reflection on UCF has been studied experimentally in Refs. [23, 131] for a two-terminal NS sample, confirming the theoretical predictions in the absence of TRS (see also [132]). Fluctuations in multiterminal samples were studied in Refs. [133, 134], where the magnitude of UCF is of the same order as that predicted in Paper I. However, the latter papers do not include a comparison between the cases in the presence and absence of superconductivity. Hence, a detailed experimental study on the effect of Andreev reflection on UCF in multiterminal samples remains to be carried out.

5 Effects far from equilibrium

The nature of equilibrium and linear-response phenomena is often known to much more detail than the corresponding true nonequilibrium effects, since their theoretical study contains a major simplifying feature: only the *spectrum* of a desired observable is needed for the evaluation of the thermal average value of the observable — or, as in many cases, one may apply analytic continuation to imaginary time and equate the observable at the discrete Matsubara frequencies.

In a nonequilibrium situation, in addition to the spectrum, also the *distribution* of quasiparticles needs to be solved for. As shown in Subs. 3.3, this is typically the solution of a Boltzmann-type kinetic equation, whose coefficients may depend on the spectral properties of the system, or even on the solution itself (as is the case with the collision integrals). A counterexample to this rule is the scattering approach, which can treat nonequilibrium effects but which relies on the existence of a local equilibrium in the reservoirs.

In small metallic wires of size L, a novel energy scale, Thouless energy ε_T [12], becomes important. It is defined as the inverse average time required to traverse through the system. In diffusive metals, $\varepsilon_T = \hbar D/L^2$ and it shows up as a natural energy scale for the superconducting proximity effect into such wires: for $\varepsilon < \varepsilon_T$, the pairing amplitude extends throughout the size L whereas for $\varepsilon > \varepsilon_T$, its decay scale is less than L. Therefore, a rule of thumb for separating between linear-response and true nonequilibrium effects in such systems is given by the comparison between ε_T and the energy scales creating the nonequilibrium, such as the one given by the voltage, eV.[17]

In this section, two examples of true nonequilibrium effects are considered. In Subs. 5.1 and in Papers V – VIII, we describe how the Josephson supercurrent through a normal-metal weak link can be controlled by inducing a nonequilibrium quasiparticle distribution from an additional normal-metal probe and, reciprocally in Subs. 5.2 and in Paper IX, how the distribution function can be controlled by the supercurrent to yield a nonequilibrium Peltier-like effect. In Subs. 5.3 and in Paper II, we show how superconducting proximity effect changes the voltage dependence of current noise. Simultaneously, these phenomena serve as examples of applications of the two theoretical approaches considered in this Thesis: nonequilibrium supercurrent is described by the real-time quasiclassical Green's-function formalism, and shot noise by the scattering approach.

5.1 Nonequilibrium supercurrent

One of the consequences of the superconducting proximity effect is the possibility to transport supercurrent through a non-superconducting medium, a weak link, placed between two superconductors. This *Josephson effect* was first predicted [18] for insulating (I) weak links. The direction and the relative magnitude of this current depends on the difference φ between the phases of the superconducting order parameters at the two

[17] If the metal is shorter than the superconducting coherence length such that $\Delta < \varepsilon_T$, the characteristic energy scale becomes Δ.

sides of the weak link. The behavior of the supercurrent in large SIS systems is fairly well known [135], but the quantum effects observed in small Josephson junctions have been recently under close scrutiny due to the suggestion of their probable use as quantum bits [136].

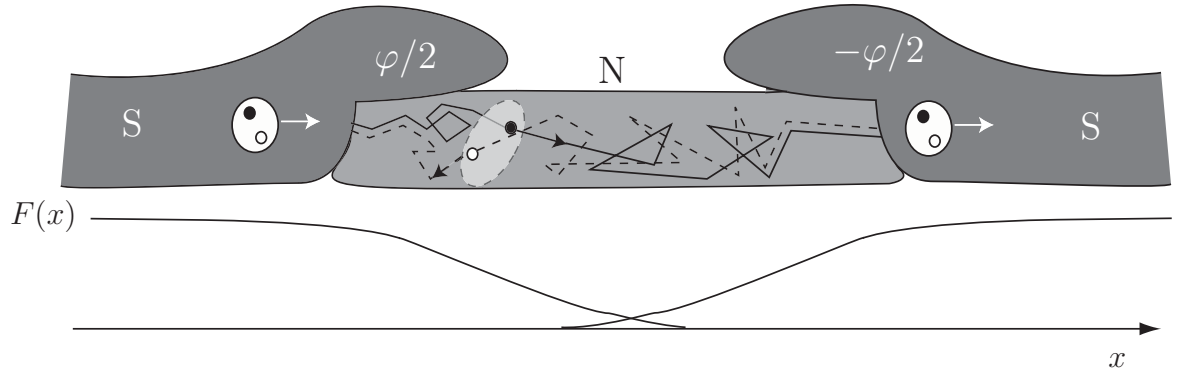

Figure 13: Superconductor-normal metal-superconductor (SNS) Josephson junction.

Metallic weak links (see Fig. 13) contain many phenomena not present in SIS junctions. There, the pairing amplitude penetrates to much greater distances than in insulators: in the latter, a typical penetration depth is a few nanometers whereas supercurrents have been observed through normal-metal weak links many microns long. The possibility to vary the length d leads to two regimes of weak links, when d is compared to the superconducting coherence length $\xi_0 \equiv \sqrt{D/2\Delta}$. In the short-junction regime $d \ll \xi_0$, the important energy scale for the temperature (or voltage) dependence of the supercurrent is the superconducting order parameter Δ [137]. For the opposite regime $d \gg \xi_0$, Δ ceases to be important, but another energy scale, the Thouless energy $E_T = \hbar D/d^2$ becomes relevant [11, 138]. The spectrum of the supercurrent-carrying states, defined below, is described in both of these regimes in Paper VII. Below, we mostly concentrate on the long-junction regime since only there a diffusive weak link can be driven into a π-state.

Physical phenomena encountered in quantum many-body systems are often based on probing the spectrum of states corresponding to the desired observable, the states being filled according to an appropriate distribution function. Variation of either the spectrum or the distribution function leads to a variation of the observable, yielding information on the system. Such a viewpoint may also be taken on the SNS supercurrent [19,139,140]. It is carried by a spectrum of states [27,141], spectral supercurrent, weighed by their distribution function. The latter can be controlled, for example, by coupling an extra normal terminal to the weak link. Varying the voltage between this terminal and the superconductors allows one to control the occupation of the current-carrying states, leading to a variation of the supercurrent. This phenomenon was experimentally first realized in Ref. [17]. The observed supercurrent can be quantitatively evaluated in terms of the diffusive-limit description of the supercurrent spectrum (Refs. [19, 142] and Paper VII), and the solution for the spatial dependence of the distribution function (Ref. [143] and Paper VI), including both elastic and inelastic effects.

Papers V – VIII study different aspects of the nonequilibrium supercurrent both theoretically (all of them) and experimentally (VI and VIII). In Paper V, we show an analogy between voltage-controlled and ferromagnetic Josephson weak links and suggest that the voltage dependence of the supercurrent in a nonequilibrium ferromagnetic weak link could be used for measuring the magnetic properties. This would also serve as a useful test for the developing theories of electronic properties of itinerant ferromagnets.

The first quantitative calculations of the supercurrent spectrum [19] applicable to the experimental systems, were carried out in an ideal two-probe geometry where the extra control wires do not affect the spectrum. Paper VII takes into account factors important in an actual quantitative comparison between the theory and the experiments. Knowing these factors facilitates the design of new experimental setups, for example, to obtain maximal control of the supercurrent by the applied voltage.

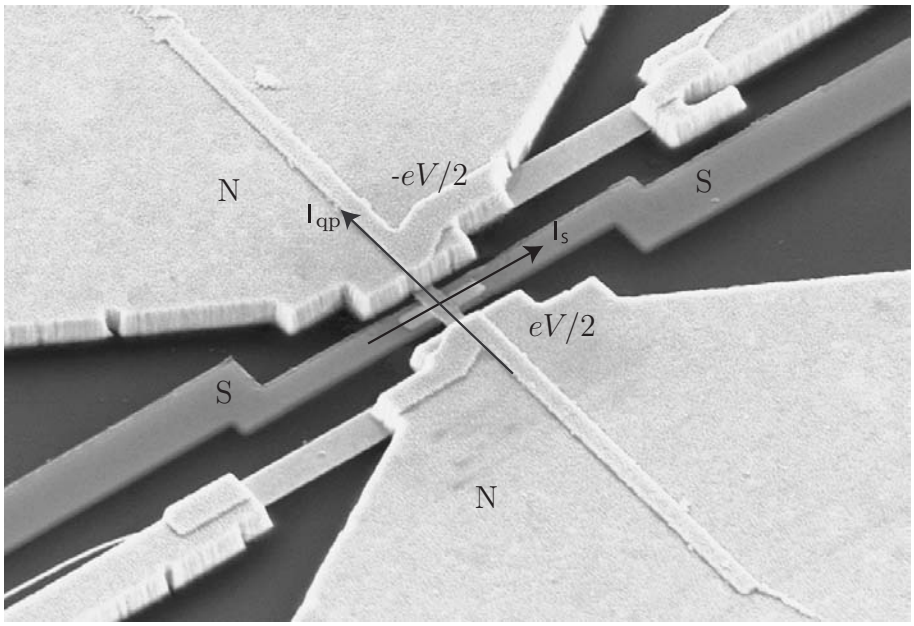

Figure 14: Four-probe controllable Josephson junction used in the experiments for Ref. [17]. The quasiparticle distribution function in the Au weak link between the two superconducting Nb wires is controlled by applying a quasiparticle current $I_{\rm qp}$ in the mesoscopic Au wire between two large Au reservoirs creating the voltage V between the latter. (Courtesy of J. Baselmans, texts and arrows added by the author.)

To avoid the effects of the (dissipative) quasiparticle current flowing in the control wires on the supercurrent, other than through the control of the local distribution function in the weak link, the first experiments separated them: whereas the previous current flows between two normal-metal reservoirs, the latter flows between the superconductors (see Fig. 14). This scheme requires at least a four-terminal setup. In Paper VI, we show that this does not need to be the case but the same phenomenon is found even if the normal and supercurrent flow in parallel, mixing with each other (see below and Paper IX for details). Therefore, one can avoid the construction of the fourth terminal and, furthermore, it can be argued that a three-terminal configuration is less vulnerable to the

presence of electron-electron scattering (see Paper VI).

One of the most striking features of the nonequilibrium-controlled supercurrent is the crossover between the conventional state of the junction to the π-state. At the crossover, these two states can coexist, leading to the supercurrent-phase dependence of the form $I_C \sin(2\varphi)$ instead of the usual $I_C \sin(\varphi)$. Such a halving of the current-phase period was measured for the first time in s-wave weak links in Paper VIII. In paper VII, we offer a qualitative physical explanation for the appearance of the higher harmonic contribution, due to a correlated transfer of a cluster of many Cooper pairs.

Below, the origin of the supercurrent-carrying states is explained on a qualitative level and it is described how one obtains the observable supercurrent from this spectrum and a nonequilibrium distribution function.

Supercurrent-carrying density of states

In a normal-metal weak link, the supercurrent is carried by a spectrum of states which correspond to quasiparticle trajectories containing an Andreev reflection at both ends of the weak link [26,27,141,144]. This spectrum can be derived in the ballistic regime from quite simple considerations and it characterizes also some properties of the supercurrent in the diffusive limit. Consider the one-dimensional NS structure discussed in Subs. 3.1, now in the case of a vanishing interface scattering $U = Z = 0$, but terminate the normal-metal wire by another semi-infinite superconductor, located at $x < -d$, with phase $\varphi_S - \varphi$ of the order parameter. The quasihole Andreev reflected from the right interface may then again Andreev reflect at the left interface, creating a quasiparticle which then traverses back to the right interface. If the total phase acquired by the quasiparticle pair during one cycle due to the dynamical phase and the phase acquired on Andreev reflection (see Table I), $\phi_{\rm tot} = 2\varepsilon d/v_F + \varphi - 2\arccos(\varepsilon/\Delta)$, is an integer multiple of 2π, a bound state is formed. And since the net result of one such cycle is the transfer of a Cooper pair from the left superconductor to the right, this bound state carries a supercurrent. For $\varepsilon_m \ll \Delta$, the bound-state condition yields the bound-state energies,

$$\varepsilon_m^{\pm} = \frac{v_F}{2d}\left(2\pi(m+\frac{1}{2}) \pm \varphi\right) \tag{58}$$

whereas for $\varepsilon_m \approx \Delta$, one needs to solve the bound-state condition numerically. The bound states corresponding to the energies ε_m^- carry current from right to left, i.e., they are composed of left-moving electrons and right-moving holes (the phase shift acquired in Andreev reflection from a quasihole state to a quasiparticle state is $-\varphi_S - \arccos(\varepsilon/\Delta)$). In this case, we obtain a spectral supercurrent expressing the magnitude of the supercurrent carried by each state from

$$j_S(\varepsilon;\phi) \propto -\sum_{\substack{m \\ \alpha=\pm}} \frac{\partial \varepsilon_m^\alpha}{\partial \varphi}\delta(\varepsilon - \varepsilon_m^\alpha), \tag{59}$$

i.e., a peak-like spectrum consisting of both positive ($\varepsilon = \varepsilon_m^+$) and negative ($\varepsilon = \varepsilon_m^-$) parts.

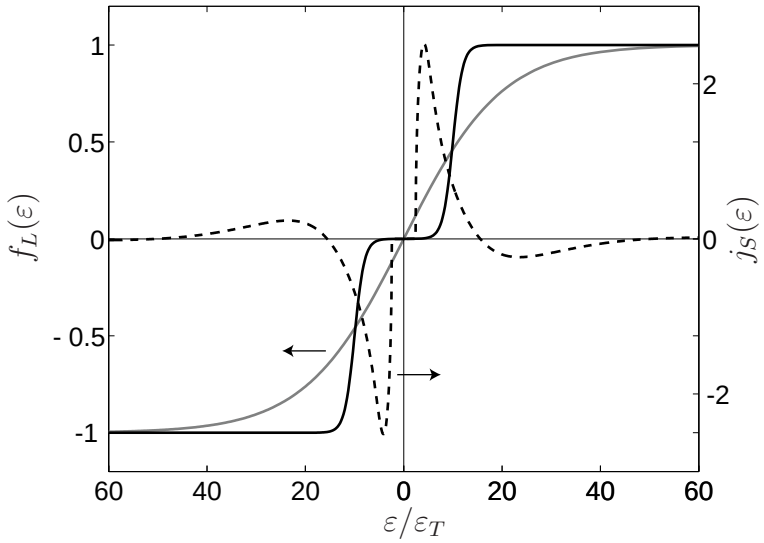

Figure 15: The observable supercurrent is obtained by integrating over the spectrum of supercurrent-carrying states (dashed, right axis), weighed by the occupation number $f_L(\varepsilon)$ of correlated particle-hole pairs (solid, left axis). An equilibrium distribution is shown in grey and a nonequilibrium distribution in the absence of inelastic effects in black.

In a diffusive weak link similar Andreev bound states are still formed, but since elastic scattering makes rise to a broad and continuous distribution of trajectory lengths between successive Andreev reflections at the two NS interfaces, also the spectral supercurrent becomes continuous. However, it still contains both such energies where supercurrent is carried in the positive direction (e.g., from left to right) as well as energies with a negative supercurrent (right to left).[18] The diffusive-limit spectral supercurrent, calculated from the quasiclassical theory with $\varphi = \pi/2$, is illustrated in the dashed line of Fig. 15.

Nonequilibrium control of the supercurrent

The observable supercurrent through a normal-metal weak link with a given phase φ is obtained by integrating over the spectrum $j_S(\varepsilon;\varphi)$ of current-carrying states, weighted by the occupation number of correlated electron-hole pairs, $f_L(\varepsilon) \equiv f(-\varepsilon) - f(\varepsilon) = 1 - (f_h(-\varepsilon) + f(\varepsilon))$, where $f_h(-\varepsilon)$ is the hole distribution function, obtained from the electron distribution by $f_h(-\varepsilon) = 1 - f(-\varepsilon)$. Therefore, breaking an electron-hole pair by creating a negative-energy hole-like or a positive-energy electron-like excitation decreases the magnitude of the supercurrent carried at energy ε. The observable supercurrent is then given as

$$I_S = \frac{\sigma_N A}{2de} \int_{-\infty}^{\infty} \mathrm{d}\varepsilon j_S(\varepsilon,\varphi) f_L(\varepsilon). \tag{60}$$

Here σ_N is the normal-state conductivity of the weak link, A its cross section and d the distance between the superconductors ($j_S(\varepsilon,\varphi)$ is chosen dimensionless). Note that in

[18] In the diffusive-limit calculations in Papers V – IX, we do not evaluate the spectral supercurrent as a diffusive limit of Andreev bound states (ABS), but rather use $j_S(\varepsilon) = \mathrm{Im}(j_E(\varepsilon))$ as in Subs. 3.3. However, ABS are responsible for the physical phenomenon underlying the calculated observable.

some cases such as equilibrium and the four-probe setup considered in Ref. [19] where $f_h(-\varepsilon) = f(\varepsilon)$, one may also write $f_L(\varepsilon) = 1 - 2f(\varepsilon)$.

The spectral supercurrent $j_S(\varepsilon)$, apart from its dependence on the phase φ, depends only on the geometry and microscopic properties of the weak link (see Paper VII), such that once the weak link is fabricated, it can no longer be varied. However, the distribution function $f_L(\varepsilon)$ depends on the state of the system, such that it can be controlled through the temperature or by creating a nonequilibrium through a voltage between extra control probes.

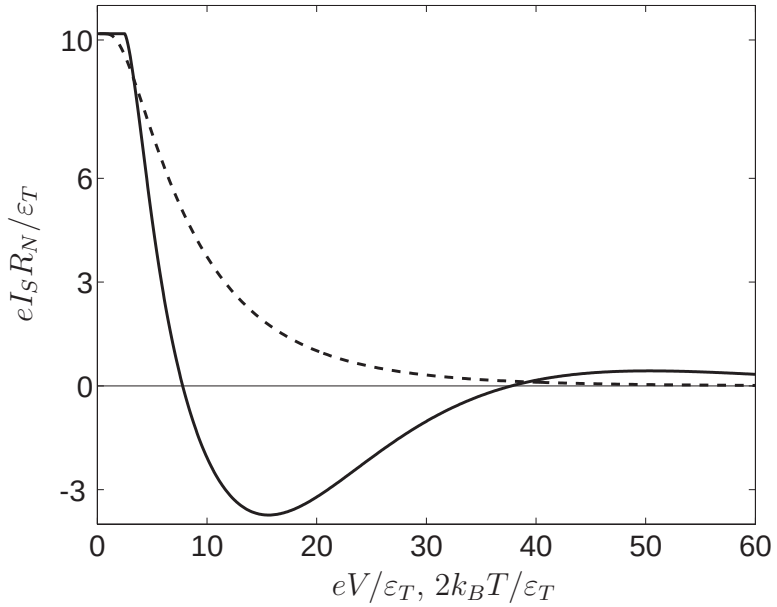

Figure 16: Voltage dependence of the supercurrent at $\varphi = \pi/2$ at a vanishing temperature $T = 0$ and in the absence of electron-electron interactions (solid line). The corresponding temperature dependence is shown for comparison (dashed).

As an example, consider the four-probe setup of Fig. 14. When the voltage V between the two normal-metal reservoirs is zero, the system is at equilibrium and $f_L(\varepsilon) = \tanh(\varepsilon/2k_BT) \equiv f_L^0(\varepsilon)$. In this case the integral in Eq. (60) can be converted to a sum over the poles ω_n of $f_L(\varepsilon)$, corresponding to the Matsubara frequencies applied in equilibrium systems[19]. Applying a voltage V symmetrically between the normal probes yields the function $f_L(\varepsilon)$ given by Eq. (19) with $\mu = eV/2$ in both reservoirs, and in the absence of inelastic scattering, this form persists into the control wires and the weak link. Defining $f_L^0 = \tanh(\varepsilon/2k_BT)$ we obtain

$$I_S = \frac{\sigma_N A}{4d} \int_{-\infty}^{\infty} \mathrm{d}\varepsilon j_S(\varepsilon) \left(f_L^0(\varepsilon + eV/2) + f_L^0(\varepsilon - eV/2) \right). \tag{61}$$

For $k_BT \ll eV/2$, $f_L(\varepsilon < eV/2) \approx 0$ and hence, spectral supercurrent from energies below $eV/2$ is blocked (see Fig. 15). At a certain voltage V, due to the oscillating nature

[19]Such a treatment is valid as long as an analytical form may be found for $f_L(\varepsilon)$. In the presence of inelastic scattering, this is seldom the case.

of $j_S(\varepsilon)$, the supercurrent for a given phase φ changes sign. In this case, the junction has turned into the π-state. The resulting voltage-dependent supercurrent at $\varphi = \pi/2$ is depicted in Fig. 16.

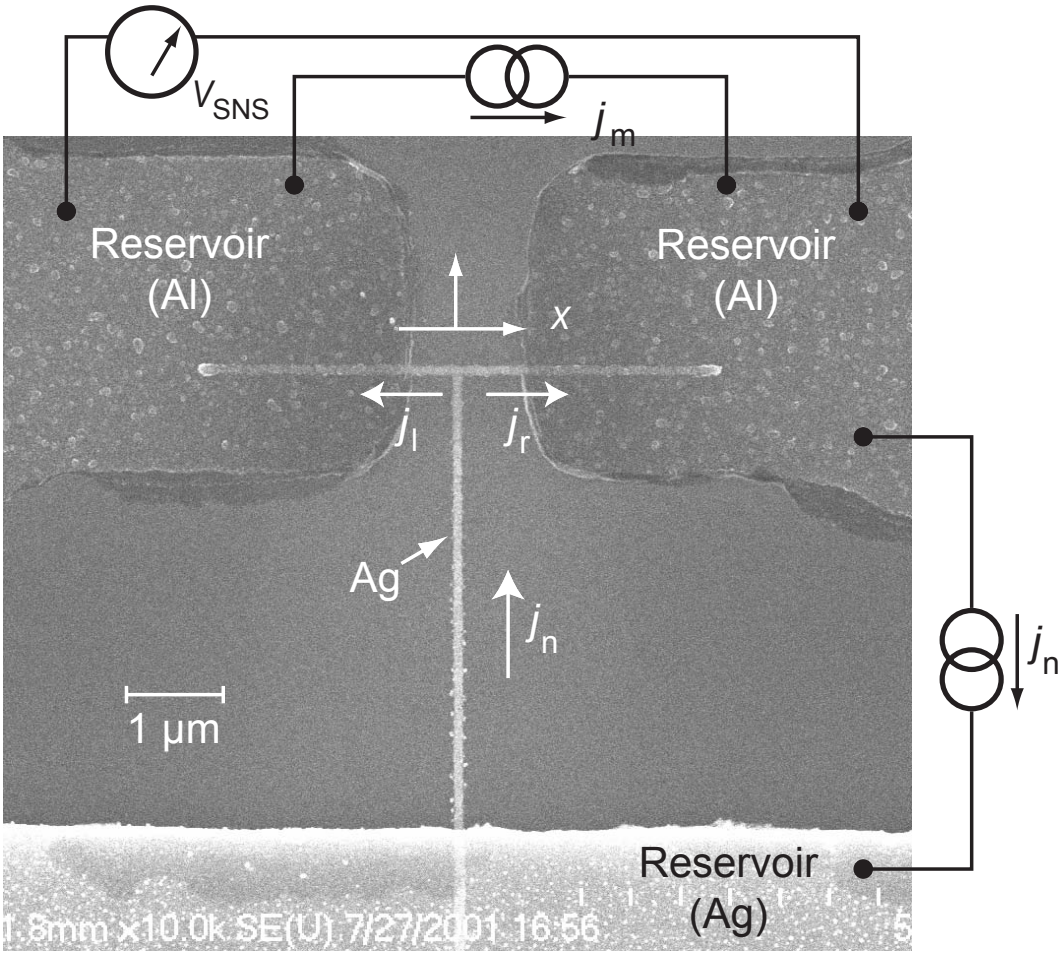

Figure 17: Three-probe structure for the study of nonequilibrium supercurrent, measured in experiments for Paper VI. (Courtesy of F. Pierre, some texts and arrows added by the author.)

In the four-probe system considered above, the quasiparticle current created by the applied voltage[20] is spatially separated from the supercurrent and thus we could obtain $f_L(x) = \text{const.}$ and also $I_S(x) = \text{const.}$ As an alternative, consider the three-probe setup of Fig. 17 studied in Paper VI. There, the quasiparticle current flows parallel to the supercurrent. According to Eq. (50), only the sum of these two is conserved. How is the supercurrent j_m flowing between the superconductors evaluated? Since the total spectral charge currents j_i ($i = m, l, r, n$, see Fig. 17) in the three arms of the structure are conserved, we can evaluate them anywhere, for example at the cross. There we have, using the continuity of spectral coefficients and the fact $j_m = j_l - j_r$

$$j_m = \mathcal{D}_T(0)(\partial_x f_T^r(0) - \partial_x f_T^l(0))/2 + j_S f_L^0(\varepsilon; V, T). \tag{62}$$

[20] In typical experiments the voltage is created by driving the quasiparticle current.

In order to show that j_m depends on j_n only through $f_L^0(\varepsilon; V, T)$ (i.e., $j_m = j_S f_L^0(\varepsilon; V, T)$), we need to show that

$$\partial_x f_T^l(0) = \partial_x f_T^r(0),$$

i.e., that the quasiparticle current is equally diverted into the two horizontal arms.

Now assume the solution of the kinetic equations (49,50) in the left horizontal arm to be the functions

$$\{f_L^l(x,\varepsilon), f_T^l(x,\varepsilon)\}. \tag{63}$$

Then it is straightforward to show that, assuming symmetric arms,

$$\{f_L^r(x,\varepsilon), f_T^r(x,\varepsilon)\} = \{2f_L^0(\varepsilon; V, T) - f_L^l(x,\varepsilon), f_T^l(x,\varepsilon)\} \tag{64}$$

is the solution of the kinetic equations in the right arm satisfying the boundary conditions. Hence, we obtain that in the three-probe case, $\partial_x f_T^l(0) = \partial_x f_T^r(0)$, i.e., the quasiparticle current is equally divided into both S arms. Furthermore, due to the absence of supercurrent in the vertical control arm, f_L stays there constant, and in particular, $f_L^l(x=0) = f_L^r(x=0) = f_L^0(\varepsilon, V, T)$. The supercurrent I_m can thus be calculated at the center of the structure by Eq. (61) as in the four-probe case. However, this example shows that whereas mixing of the two kinds of currents is not important for the critical current (in the absence of interactions), it does drastically change the behavior of the distribution functions in the horizontal arms. This phenomenon is discussed in the following subsection.

Supercurrent through a ferromagnet

As mentioned in the previous section, heterostructures composed of weak ferromagnets and superconductors may be described theoretically through the term $h\hat{\tau}_3 \otimes \hat{\sigma}_3$ due to the exchange field. In the ferromagnet, this makes the parametrized Usadel equation take the form (for simplicity, assuming translational invariance in y- and z-directions)

$$\begin{aligned} D\partial_x^2\theta &= -2i(\varepsilon \pm h)\sinh(\theta) + \frac{1}{2}\left(\partial_x\chi\right)^2 \sinh(2\theta) \\ j_E &= -\sinh^2(\theta)\partial_x\chi, \quad \partial_x j_E = 0. \end{aligned} \tag{65}$$

The term $+h$ corresponds to the combination of an electron with spin $\uparrow$ and hole with spin $\downarrow$ and vice versa for $-h$. Finally, the observables are summed over these two combinations. For example, the equilibrium supercurrent becomes

$$I_S = \frac{\sigma_N A}{4d}\int_{-\infty}^{\infty} \mathrm{d}\varepsilon \left(j_S(\varepsilon + h) + j_S(\varepsilon - h)\right) f_L^0(\varepsilon). \tag{66}$$

In the first term, shifting the variable of integration by $-h$ and in the second, by h, yields the same form as in Eq. (61), but where $eV/2$ is replaced by h.[21] Therefore, the supercurrent through a weak ferromagnet (where $h \ll \Delta$), first described in Refs. [102,

[21] For $h \gtrsim \Delta$, this is not strictly valid since the exchange field does not penetrate into the superconductors - such an analogy would apply better in the case of Zeeman splitting in an in-plane magnetic field.

145], is formally analogous to the nonequilibrium controlled supercurrent, in the absence of interactions. This analogy has been pointed out in Ref. [146] and in Paper V.

The analogy suggests that we can combine these two effects (as discussed in Paper V and, independently, in Ref. [147]) by replacing the normal-metal wire, for example in Fig. 14, by a weak ferromagnet. As a result, one obtains four terms,

$$I_S(h;V) = \frac{1}{4}\big[I_S(h+eV/2) + I_S(h-eV/2) + I_S(-h+eV/2) + I_S(-h-eV/2)\big], \quad (67)$$

where the first argument of I_S tells the magnitude of the effective exchange field and the second (if present) the control voltage. Thus, the supercurrent separates into four parts, due to terms with combinations of electrons and holes with opposite spins coming from the two reservoirs. Let us assume that $h \gg E_T$, such that $I_S(h)$ is exponentially suppressed. Tuning the voltage such that $V = 2h/e$, two of the terms in Eq. (67) yield $I_S(\pm 2h)$, and two $I_S(0)$. Since the first of these are very small and may be neglected but the second do not contain the large field h, we simply obtain a supercurrent half of the original one, *without the effects of the exchange field and voltage*. Therefore, the nonequilibrium can be used to recover the exchange-field suppressed supercurrent, and since $I_S(h;V)$ obtains a maximum at $V = 2h/e$, this effect can be used to measure the exchange field or Zeeman splitting in the weak link.[22]

Correlated transport of multiple Cooper pairs

Within n cycles, the Andreev bound states carry the total of n Cooper pairs through the weak link in a correlated fashion. An alternative way to consider this phenomenon is a transport of a group of n Cooper pairs, with the total phase $n\varphi$. Each such a group yields a supercurrent proportional to $\sin(n\varphi)$ such that the total supercurrent can be written as a Fourier series,

$$I_S(\varphi) = \sum_{n=1}^{\infty} I_{C,n} \sin(n\varphi), \quad (68)$$

where $I_{C,n}$ is the amplitude for carrying n correlated Cooper pairs through the weak link. In the ballistic case, each additional cycle adds $2d$ to the total length of the quasiparticle trajectory. Therefore, the amplitudes decay as $I_{C,n} \propto 1/n$, yielding a sawtooth total current-phase dependence [139].

In the case of a tunneling weak link, the probability for a correlated transfer of multiple Cooper pairs is much smaller than for a single pair, and hence one obtains the usual SIS current-phase relation $I_S = I_C \sin(\varphi)$. In the diffusive case, the probability for transferring clusters of multiple Cooper pairs is finite, and therefore, the current-phase relation deviates from the sinusoidal one especially at low temperatures (see, e.g., Refs. [11,137]). Also the spectral supercurrent $j_S(\varepsilon)$ can be written as a Fourier sin-series and one finds (see Paper VII) that at low temperatures, at least the few first harmonics can in principle be observed. Since the control voltages V_n^* where the amplitudes $I_{C,n}(V_n)$ change sign

[22] This picture is idealized: we assumed $h \ll \Delta$ and no electron-electron interactions deforming the distribution function. However, we expect that traces of this effect can be seen even for $h \lesssim \Delta$, and with short control wires compared to the electron-electron scattering length.

depend on the index n, the point $V = V_1^*$ where the first harmonic is suppressed may still contain finite higher-harmonic contributions. Therefore, around the crossover voltage V_1^*, the critical current, i.e., the maximum observable supercurrent, does not totally vanish, but the maximum is obtained at a phase different from $\pi/2$. The current-phase dependence around the crossover voltage V_1^* was studied experimentally and theoretically in Paper VIII, confirming the phase dependence $I_S \approx I_{C,2}\sin(2\varphi)$ around this voltage. The analysis of the free energy of the junction in this case shows that around V_1^*, the junction has two energy minima, at $\varphi = 0$ and at $\varphi = \pi$, with a degeneracy at $V = V_1^*$. A similar behavior of higher harmonics in the Josephson current-phase relation has been observed in $YBa_2Cu_3O_{7-x}$ grain boundary junctions [148] due to the d-wave pairing of the order parameter.

5.2 Tuning distribution functions with supercurrent

In the previous subsection, we described how the supercurrent through a normal-metal weak link can be tuned by varying the quasiparticle distribution function via additional normal-metal probes. The three-probe setup, where the quasiparticle current and supercurrent flow in parallel, shows that in the "horizontal" wires (see Fig. 17), the nonequilibrium distribution functions themselves depend on the supercurrent. This dependence is studied in Paper IX, where we show that supercurrent may induce large nonequilibrium thermoelectric effects. The kinetic equations (50) show that in a nonequilibrium situation, supercurrent contributes to the energy flow the term $\varepsilon j_S f_T(x)$. As this energy flow cannot pass to the superconductors, it has to be counterbalanced by another energy flow, driven by the gradient of the asymmetric distribution function, $\varepsilon\mathcal{D}_L\partial_x f_L$. As a result, the charge nonequilibrium described by f_T is mediated to an energy nonequilibrium.

The kinetic equations (50) cannot in general be solved in closed form — there exists no analytical solution even for the kinetic coefficients. In most cases, one has to focus on a numerical solution of both spectral (for the retarded and advanced functions which yield the kinetic coefficients) and kinetic (for the distribution functions) equations. One can, however, extract some symmetry properties of the distribution functions, such as those given by Eqs. (63, 64). In the absence of a supercurrent, both the local chemical potential (expressed through $f_T(x)$) and the local effective temperature (expressed through $f_L(x)$) are left-right symmetric. Passing a supercurrent through the horizontal arms retains the symmetry of $f_T(x)$, but makes an asymmetric change to $f_L(x)$.

The numerically evaluated full distribution function $f(\varepsilon, x)$ in the two arms is plotted in Fig. 18 in the absence of supercurrent and in Fig. 19 for phase difference $\varphi = \pi/2$ yielding nearly the maximum supercurrent. The major change shows up in the antisymmetric part $f_L(\varepsilon)$ of the distribution function, reflecting the counterbalancing of the energy flow carried by the supercurrent in the nonequilibrium state. The supercurrent induces a small space-dependent variation $\delta\mu_{\rm eff}(x)$ in the chemical potential, mostly due

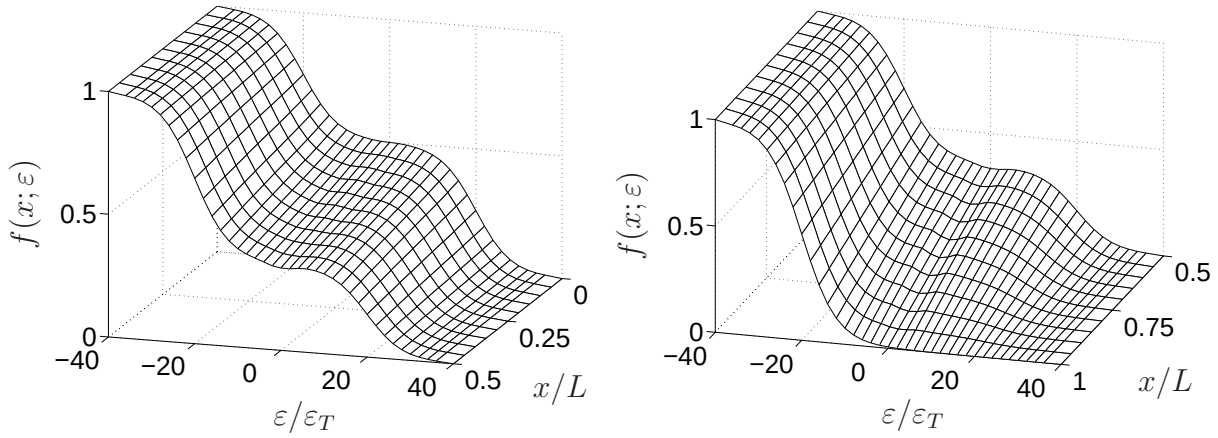

Figure 18: Quasiparticle distribution function in the three-probe case, Fig. 17 (assuming each arm to be of length $L/2$), in the absence of supercurrent (phase difference $\varphi = 0$). The behavior in the two horizontal arms ($x = 0 \dots L/2$) is shown on the left, and in the vertical arm ($x = L/2 \dots L$) on the right. For a left-right symmetric setup, the distribution function is the same in both horizontal arms. The proximity effect on the kinetic coefficients is present, but can mostly be seen in the space and energy derivatives of the distribution functions (cf. Fig. 6 where we assumed no proximity effect). The energies are plotted as a function of the Thouless energy ε_T corresponding to the length L, and the voltage and the temperature are $V = 20\varepsilon_T/e$ and $T = 4\varepsilon_T/k_B$.

a) b)

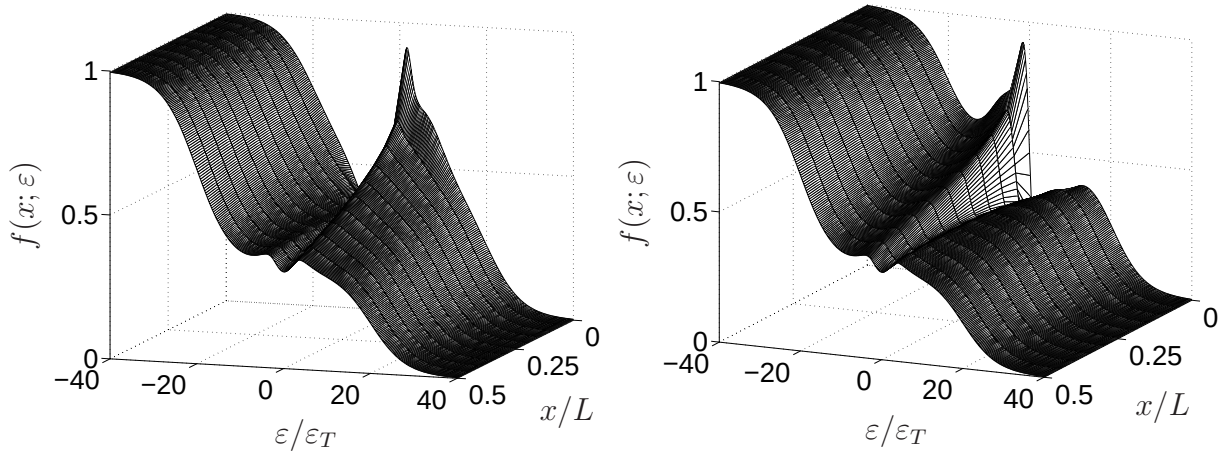

Figure 19: Quasiparticle distribution function in the horizontal arm of the three-probe case, Fig. 17, in the presence of supercurrent (phase difference $\varphi = \pi/2$): a) left horizontal arm, b) right horizontal arm.

to the fact that the kinetic coefficients are altered by the supercurrent, but a more

dramatic change is induced in the effective temperature $T_{\rm eff}$. This can be expressed as

$$T_{\rm eff}(x) = \sqrt{T_{\rm eff}^0(x)^2 + S(x;V) + 3\delta\mu_{\rm eff}(x,\varphi)^2/\pi^2 k_B^2}. \tag{69}$$

Here $T_{\rm eff}^0(x)$ is the local effective temperature in the absence of the supercurrent (see Paper IX) and $S(x;V)$ characterizes the supercurrent-induced change in $f_L(x)$, given by

$$S(x;V) = \frac{6}{\pi^2 k_B^2}\int_0^\infty \varepsilon\big(f_L(x;\varepsilon) - f_L^0(\varepsilon;V)\big)\mathrm{d}\varepsilon. \tag{70}$$

The asymmetry of the supercurrent-induced variation of $f_L(x)$ implies that $S(x;V)$ is asymmetric between the two wires, increasing the temperature in the left arm and decreasing it in the right arm. This phenomenon is similar to the Peltier effect, but much larger than typically expected for metals.

In metals, thermoelectric effects such as the Peltier effect usually rely on electron-hole symmetry breaking and are thus very small, of the order of $(k_BT)^2/E_F$, whereas here, we assume complete electron-hole symmetry. However, Eom *et al.* [149] measured another thermoelectric effect, the thermopower Q in an Andreev interferometer, a mesoscopic normal-metal wire doubly connected to a superconductor which forms a loop. Varying the magnetic field through the loop and thus the phase difference φ of the order parameters at the NS interfaces, they observed large-amplitude oscillations of Q as a function of φ. Although the measured variable and the setup were slightly different, the underlying mechanism — coupling of distribution functions through the supercurrent — is presumably the same as considered in Paper IX. Hence, our results may partially explain the findings in Ref. [149]. The thermopower in an Andreev interferometer has been theoretically studied in the regime of high tunnel barriers and within linear response in Ref. [150], leading also to an unexpectedly large effect. However, besides minor corrections, there the distribution functions are assumed in quasi-equilibrium and the transport is essentially driven by the discontinuities at the tunneling barriers.

The large effect predicted above and in Paper IX resembles a phenomenon studied in the turn of 1980's in bulk superconductors [151–154]. There, a temperature gradient along with a supercurrent generates a charge imbalance in the superconductor (which may be described through f_T). Technically, this may be explained by inspection of Eq. (50) in a superconductor, assuming that $\partial_x f_T \approx 0$. There, the gradient of f_L couples through the term $\mathcal{R}f_T$ to the symmetric distribution function f_T. In the present case, we apply Eq. (49) and couple a "charge imbalance", described by $f_T \neq 0$, through a supercurrent to a temperature gradient in a mesoscopic system.

In most of the discussion in this and the preceding subsection, we have neglected the effects of inelastic scattering. In the quantitative fits to the experimental results in Papers VI and VIII, this have to be taken into account. Typically, such effects blur the nonequilibrium effects, but taking them quantitatively into account and comparing to experiments may yield important information on their strength. Such an approach was taken in Ref. [16], where the local distribution function in a normal-metal wire between two N reservoirs was measured in a tunnelling measurement. In the three-probe case with the mixing of the quasiparticle current (controlled by the external voltage) and

the supercurrent (controlled by the phase difference between the superconductors), one obtains an extra control parameter, the supercurrent, which may make the extraction of the details of the interactions simpler. However, at present no quantitative theory of the effect of the superconducting proximity on the inelastic collision integrals exists.

5.3 Nonlinear effects in current noise

In addition to the time-averaged steady flow, the electronic current fluctuates in time. The fluctuations, current noise, at finite temperatures are partly due to the thermal noise, fundamentally connected to dissipation through the fluctuation-dissipation theorem [80]. In mesoscopic wires in the absence of inelastic scattering, also another noise term, shot noise, appears and at a vanishing lattice temperature, it is the only source of noise. This noise component reflects the discreteness of the charge carriers and it vanishes in the classical limit of a macroscopic conductor [57]. Current noise is one of the main obstacles in the quantum-mechanical manipulations of condensed-matter structures [136, 155] leading to decoherence, ultimately destroying quantum-mechanical superpositions and entanglement. However, especially shot noise can also reflect many features of the systems under scrutiny, some of which may not be present in the conductance [57]. In this subsection and in Paper II, we discuss the behavior of current noise in diffusive metallic wires, and especially study how the superconducting proximity affects the noise.

The shot noise in diffusive metallic wires both in the presence and in the absence of Andreev reflection can be described by the incoherent semiclassical Boltzmann-equation approach where the noise is described by a random Langevin source [30, 34] or by the scattering-matrix approach [156, 157]. In the linear-response regime where the latter can be accompanied with the arsenal of the random matrix theory, these two very different methods yield the same results, indicating that, in the lowest order, phase-coherent effects are not important at linear response.

The nonlinear-response shot noise in the presence of the superconducting proximity effect cannot be described by the semiclassical approach and the random-matrix theory predictions do not exist in this regime. Paper II describes these nonlinear effects by the numerical scattering approach, studying how the proximity effect changes the current noise.

Current noise is characterized by its spectral density or power spectrum $S(\omega, t)$, which is the Fourier transform of the current-current correlation function

$$S(\omega, t) = \int \mathrm{d}t' e^{i\omega t'} \langle \delta\hat{I}(t+t')\delta\hat{I}(t) + \delta\hat{I}(t)\delta\hat{I}(t+t')\rangle. \tag{71}$$

Here $\delta\hat{I}(t) \equiv \hat{I}(t) - \langle\hat{I}(t)\rangle$ describe the fluctuations in the current and the brackets denote an impurity average and an average over the state of the system. Below and in Paper II, we only consider the fluctuations in a time independent system and in the zero-frequency limit, i.e.,

$$S(\omega = 0) = 2\int \mathrm{d}t \langle \delta\hat{I}(t)\delta\hat{I}(0)\rangle. \tag{72}$$

Typically the frequency dependence becomes important if ω is of the same order as the dynamic energy scales in the studied systems, e.g., Thouless energy ε_T.

In the linear regime, the zero-frequency shot noise is typically directly proportional to the time-averaged current. A characteristic quantity for the description of shot noise in different types of materials is the Fano factor F. It is defined as the ratio between the zero-frequency shot noise and the time-averaged current I, such that

$$S = 2eFI. \tag{73}$$

In many cases, F depends only on the type of the system, not on its microscopic details. For example, for the tunneling current through an insulator, $F = 1$, and in a diffusive normal-metal wire, one obtains $F = 1/3$ (as shown below). It also reflects the type of charge carriers: for example, at an NS contact F is doubled indicating the fact that charge is carried by units with double electronic charge.

In the semiclassical theory, the zero-frequency noise for a mesoscopic wire of length L, cross section A and normal-state conductivity σ_N can be found from [34, 35, 158]

$$S = \frac{4A\sigma_N}{L^2} \int_{-\infty}^{\infty} \mathrm{d}\varepsilon \int_0^L \mathrm{d}x f(x,\varepsilon)(1 - f(x,\varepsilon)), \tag{74}$$

assuming translational invariance in the transverse (y, z) directions and that the current flows in the x-direction. Substituting the calculated distribution functions from Eqs. (17,20) in the limit $T = 0$ yields in a diffusive normal wire connected to two normal-metal reservoirs

$$S = \frac{2A\sigma_N}{3L}\mu = \frac{2e}{3}I \tag{75}$$

and connected to a normal and a superconducting reservoir,

$$S = \frac{4A\sigma_N}{3L}\mu = \frac{4e}{3}I. \tag{76}$$

In the latter $eV < \Delta$ was assumed. Thus, we have in the normal case, $F = 1/3$. In the presence of Andreev reflection, the Fano factor is doubled to $F = 2/3$.

In the scattering approach, noise can be obtained from the elements of the scattering matrix s similarly as in Subs. 3.2 in the case of conductance. The shot noise is expressed in terms of the eigenvalues of different parts of s, in the spin-degenerate normal case it is given through the transmission eigenvalues T_n [57],

$$S_{\mathrm{N}} = \frac{4e^2}{h} \int_0^{eV} \mathrm{d}\varepsilon \sum_n T_n(\varepsilon)(1 - T_n(\varepsilon)). \tag{77}$$

In the case of an NS interface the sub-gap shot noise can be related to the Andreev-reflection eigenvalues $R_{A,n}$ via [156, 157]

$$S_{\mathrm{NS}} = \frac{16e^2}{h} \int_0^{eV} \mathrm{d}\varepsilon \sum_n R_{A,n}(\varepsilon)(1 - R_{A,n}(\varepsilon)). \tag{78}$$

In the linear response, we only need to find the scattering-matrix elements at the Fermi level and thus we get

$$S_{\mathrm{N}} = \frac{2e^3V}{h} \sum_n T_n(1 - T_n) \tag{79}$$

$$S_{\mathrm{NS}} = \frac{8e^3V}{h} \sum_n R_{A,n}(1 - R_{A,n}) \tag{80}$$

If the transmission eigenvalues T_n do not depend on energy, i.e., in the linear-response limit, we may apply the random matrix theory to find their distribution in the diffusive limit [59]. This is given by

$$\rho(T) = \frac{h}{2e^2 R_N} \frac{1}{T\sqrt{1-T}}, \tag{81}$$

where R_N is the resistance of the mesoscopic wire. Integrating Eqs. (34,79) over the transmission eigenvalues weighed by their distribution directly yields $S = 2eG_N V/3$, i.e., the Fano factor $F = 1/3$. A similar procedure may be carried out in the NS case, at $\varepsilon = 0$. In this case, the Andreev-reflection amplitudes $R_{A,n}$ may be related to the normal transmission amplitudes T_n through the diffusive N wire [55], such that (at a vanishing magnetic field)

$$R_{A,n} = \frac{T_n^2}{(2-T_n)^2}. \tag{82}$$

Substituting this relation into Eqs. (35,80) yields $G_{\rm NS} = G_{\rm N}$ and $S_{\rm NS} = 2S_{\rm N}$, i.e., the same as given by the semiclassical approach.

Nonlinear-response noise in the presence of the superconducting proximity effect, i.e., in a NS wire with eV exceeding the Thouless energy, cannot be described by a semiclassical Boltzmann-Langevin approach. Also the analytical scattering approach with the random matrix theory can no longer be applied, since Eq. (82) is strictly valid only with $\varepsilon = 0$. Such nonlinear effects were measured in recent experiments [22, 159], which also confirmed the doubling of noise in the linear regime. A numerical scattering-matrix study of the nonlinear effects is given in Paper II. It shows that at nonlinear response, shot noise becomes voltage dependent, following the (nonlinear) voltage dependence of the time-averaged current.

Recently, a quasiclassical method for the study of the current fluctuations has been developed [69]. This method is not only suited for the study of the current noise, defined as the second moment of current fluctuations, but it can describe all its moments. The numerical results obtained using this approach for the description of proximity affected noise in a diffusive NS contact are in agreement with the results of Paper II.

With the enhanced resolution in experiments, shot noise is turning from an unwanted obstacle towards an important observable. To obtain a comprehensive understanding of the nonlinear effects superconductivity has on the noise, both methods based on quasiclassical formalism and the scattering approach are required.

6 Discussion

This dissertation discusses physical phenomena taking place in phase-coherent metallic conductors in contact to superconductors and the theory constructed for their description. The basic phenomena responsible for the effects of superconductivity are the proximity effect, i.e., the penetration of the superconducting order parameter into the normal-metal side, and Andreev reflection. These effects are closely related but not exactly two sides of the same coin: the overall magnitude of the proximity effect depends on that of Andreev reflection, but its penetration depth is determined by the properties of the metal into which it penetrates. On the other hand, even if the proximity effect is limited only into the vicinity of the interface such that most of the normal-metal wire does not show induced superconductivity, the presence of Andreev reflection affects the form of quasiparticle distribution functions throughout the normal-metal wire.

The dissertation focuses on the study of the proximity effects (i) in heterostructures of superconducting and ferromagnetic material, on the effect of superconductivity (ii) on the fluctuations of the linear conductance of mesoscopic wires and (iii) on the fluctuations of currents in time, and, as a major part, (iv) on nonequilibrium supercurrent in controllable weak links and (v) on supercurrent-induced nonequilibrium thermoelectric effects. Except for the inverse proximity effect due to ferromagnetism, the phenomena considered essentially take place in the normal-metal side, and superconducting features found in these wires are induced by the nearby superconductors. The main results of this work and some of the open problems are summarized below.

(i) **Superconductor-ferromagnet (SF) heterostructures**
Superconductors and ferromagnets fabricated in close contact with each other exhibit mutual proximity effects due to their ordered nature. In most cases, superconducting proximity effect is strongly suppressed by the ferromagnet, and the magnetic proximity effect, penetration of spin polarization, has not been observed. Therefore, as indicated in Paper IV, the strongest effect in the superconducting side is the inverse proximity effect induced by the suppression of the pairing amplitude in the ferromagnet. Observations of long-range effects in the ferromagnetic side still need to be clarified. The local density of states, indicating the extent of the mutual proximity effects, was measured in Paper IV using a normal-metal tunnel probe. For a complete study of the possible magnetic proximity effect, a ferromagnetic probe should be used.

Placing a low-T_{Curie} ferromagnet between two superconductors allows to transport supercurrents through this ferromagnetic weak link. At certain values of temperature and exchange field, these junctions turn into the π-state [117]. In Paper V, we show how, with a temperature independent exchange field, the crossover between the conventional and π-states can take place as a function of temperature. We also show that formally, the π-state formed in a SFS junction has the same origin as that formed in a nonequilibrium-controlled junction [17]. Combining the effects of nonequilibrium and ferromagnetism in a suitable range of parameters, one can, for example, study the strength of the ferromagnetic exchange field.

Combining both conventional and π-junctions in an array, one can construct an intrinsically frustrated system where supercurrents flow spontaneously [160]. It has been suggested that such arrays could be used for quantum computing [20, 161].

(ii) **Andreev reflection and universal conductance fluctuations**
In Paper I, we numerically study conductance fluctuations (CF) in multiterminal samples, where current flows between two normal-metal reservoirs, but the mesoscopic wire is connected to further, superconducting reservoirs which induce Andreev reflection. It is shown that such fluctuations are universal, independent on the average conductance. Andreev reflection in these systems is shown to decrease the fluctuations, whereas for NS contacts, CF are typically increased compared to the purely normal samples. An analytical study of fluctuations in such Andreev interferometers is lacking. A field-theoretical approach has been constructed for studying the fluctuations around the solution to the Usadel equation [162]. This could in principle be applied for the study of universal conductance fluctuations in multiterminal systems.

(iii) **Proximity effect on shot noise**
Besides being an unwanted obstacle in quantum manipulations of condensed-matter systems, shot noise S can serve as a spectroscopic tool for characterizing mesoscopic structures. In Paper II, we show that in the presence of the proximity effect, for voltages V of the order of the Thouless energy ε_T/e, S becomes a nonlinear function of V. Using a numerical scattering approach, we find that S exhibits similar reentrance and reflectionless tunnelling effects as the time-averaged current [4]. Our findings are in agreement with the numerical results of the recently developed quasiclassical counting-field technique [69]. An analytical evaluation of the observed effects has not yet been carried out.

(iv) **Nonequilibrium supercurrent**
Major part of the Papers in this Thesis, V – IX, deals with nonequilibrium effects in supercurrent and controllable weak links. The supercurrent through a normal-metal weak link may be expressed as a convolution between a spectrum of supercurrent-carrying states and a distribution function. Paper VII describes how the spectrum depends on the measurement setup, thereby helping to optimize the construction of the samples. Connecting additional normal-metal reservoirs to the weak link through mesoscopic wires allows one to control the quasiparticle distribution function with an applied voltage, and thereby vary the critical current of the weak link. Paper VI shows that such a control is possible also if the supercurrent is allowed to mix with a quasiparticle current driven through the control wires.

The detailed shape of the distribution functions depends on the various scattering mechanisms in the sample, for example due to electron-electron interaction, and these need to be taken into account in a quantitative comparison between the theory and experiments. Conversely, such a comparison may yield information about the strengths of these scattering mechanisms. However, a theoretical treatment of the

proximity effect on the interactions themselves still remains to be accomplished — in Papers VI and VIII, normal-state collision integrals are applied. In the case of the equilibrium supercurrent, the quasiclassical theory and the experiments are in an excellent agreement even without the inclusion of such interaction effects [11]. Therefore, it seems that the largest effect of these scattering mechanisms is encountered in distribution functions, not in the spectral supercurrent.

One of the consequences of the nonequilibrium tuning is the fact that with certain control voltages, the π-state may become energetically more favourable than the conventional state of the weak link. In the π-state the phase across the weak link is π in the absence of supercurrent flow, and the direction of the supercurrent at a given phase is reversed. Around the crossover from the conventional to the π-state, both of these yield free-energy minima, and the resulting supercurrent-phase relation has a dominant second harmonic $\sin(2\varphi)$ component. The crossover regime was measured in Paper VIII for the first time in Josephson junctions with conventional (s-wave) superconductors. At low enough temperatures, this regime of voltages could be used to study possible hysteretic effects in these junctions or even quantum superpositions, and the effect of the quasiparticle current noise on this behavior. The use of such junctions (or SQUIDS with controllable Josephson junctions) as quantum bits working in the phase regime [21] would be limited by the dissipative control currents acting as noise sources. The strength of the induced decoherence due to this noise requires further study.

(v) **Proximity effect and thermoelectrics**

In normal metals, thermoelectric coefficients typically are very small since they depend on the nonlinearities in the quasiparticle dispersion relation (i.e., electron-hole symmetry breaking). These variations typically take place at scales of the order of ε_F, and thus the effects are of the order of k_BT/ε_F. The presence of Andreev reflection changes the usual relations between the thermoelectric coefficients, for example Wiedemann-Franz law [24] and Mott's law (Paper III), but its presence alone is not enough to make the thermoelectric effects essentially stronger.

In Paper IX, we show that the presence of supercurrents can lead to large thermoelectric effects. There, we discuss a nonequilibrium Peltier effect: supercurrent tunes the space-dependent distribution functions such that the local effective temperature can be driven in a normal-metal weak link between two superconductors. Such a large thermoelectric effect has been observed in mesoscopic normal-metal structures as a function of the phase difference between two superconductors connecting to the normal wires. Our findings indicate a qualitative explanation for these observations. The predicted Peltier effect could also presumably be used for electronic cooling at low temperatures.

At low temperatures, the space dependence of the distribution functions is strongly affected by the electron-electron interactions. In recent experiments [16, 28], these have been measured in a normal-metal wire through tunnel measurements by varying the voltage across the wire. Typically, the different scattering mechanisms are

difficult to separate from each other. Our findings yield another control parameter for this study, the supercurrent.

In nanoelectronics of the near future, the wide-scale applications and contemporary basic research on quantum phenomena are set to meet as the size of the devices continues to shrink. The quantum-mechanical properties of these systems, such as the phase coherence of electrons or the quantization of charge, may on the one hand limit the performance of the tiny devices, but can, on the other hand, be applied in a novel way in the fabrication and use of new kinds of devices. Prime examples of the latter are some of the most prominent suggestions for the quantum bit, based on the use of the phase-coherent Josephson effect in a single-electron device or in superconducting arrays of loops containing conventional and π-junctions. Such quantum engineering targets at a fine control of quantum-mechanical phenomena in condensed-matter structures. With the detailed knowledge of the supercurrent spectrum and of the nonequilibrium distribution functions, tunable Josephson junctions are starting to fulfill this goal

Phase-coherent nanostructures are also intriguing for basic physics research. The interest does not lie only on the device properties themselves, but also on the fact that they can be used to test fundamental solid-state theories, such as that on interactions in metals, and to demonstrate many basic physical principles, such as universality, symmetry, scaling and quantum phase transitions.

References

[1] P. G. de Gennes, *Superconductivity of metals and alloys* (W. A. Benjamin, New York, 1966).

[2] M. Tinkham, *Introduction to Superconductivity*, 2nd ed. (McGraw-Hill, Inc., Singapore, 1996).

[3] B. Pannetier and H. Courtois, J. Low Temp. Phys. **116**, 187 (1999).

[4] C. J. Lambert and R. Raimondi, J. Phys.: Condens. Matter **10**, 901 (1998).

[5] W. Belzig, F. K. Wilhelm, C. Bruder, G. Schön, and A. D. Zaikin, Superlatt. Microstruct. **25**, 1251 (1999).

[6] A. F. Andreev, J. Exptl. Theoret. Phys. **46**, 1823 (1964), [Sov. Phys. JETP **19**, 1228 (1964)].

[7] P. Charlat, H. Courtois, P. Gandit, M. D., A. F. Volkov, and P. B., Phys. Rev. Lett. **77**, 4950 (1996).

[8] W. Belzig, C. Bruder, and G. Schön, Phys. Rev. B **54**, 9443 (1996).

[9] S. Guéron, H. Pothier, N. O. Birge, D. Esteve, and M. H. Devoret, Phys. Rev. Lett. **77**, 3025 (1996).

[10] P. Visani, A. C. Mota, and P. A., Phys. Rev. Lett. **65**, 1514 (1990).

[11] P. Dubos, H. Courtois, B. Pannetier, F. K. Wilhelm, A. D. Zaikin, and G. Schön, Phys. Rev. B **63**, 064502 (2001).

[12] D. J. Thouless, Phys. Rev. Lett. **39**, 1167 (1977).

[13] R. J. Soulen Jr, J. M. Byers, M. S. Osofsky, B. Nadgorny, T. Ambrose, S. F. Cheng, P. R. Broussard, C. T. Tanaka, J. Nowak, J. S. Moodera, A. Barry, and J. M. D. Coey, Science **282**, 85 (1998).

[14] M. Giroud, H. Courtois, K. Hasselbach, D. Mailly, and B. Pannetier, Phys. Rev. B **58**, R11872 (1998).

[15] V. T. Petrashov, I. A. Sosnin, I. Cox, A. Parsons, and C. Troadec, Phys. Rev. Lett. **83**, 3281 (1999).

[16] H. Pothier, S. Guéron, N. O. Birge, D. Esteve, and M. H. Devoret, Phys. Rev. Lett. **79**, 3490 (1997).

[17] J. J. A. Baselmans, A. F. Morpurgo, B. J. van Wees, and T. M. Klapwijk, Nature **397**, 43 (1999).

[18] B. D. Josephson, Phys. Lett. **1**, 251 (1962).

[19] F. K. Wilhelm, G. Schön, and A. Zaikin, Phys. Rev. Lett. **81**, 1682 (1998).

[20] L. B. Ioffe, V. B. Geshkenbein, M. V. Feigel'man, A. L. Fauchère, and G. Blatter, Nature **398**, 679 (1999).

[21] J. E. Mooij, T. P. Orlando, L. Levitov, L. Tian, C. H. van der Wal, and S. Lloyd, Science **285**, 1036 (1999).

[22] X. Jehl, M. Sanquer, R. Calemczuk, and D. Mailly, Nature **405**, 50 (2000).

[23] K. Hecker, H. Hegger, A. Altland, and K. Fiegle, Phys. Rev. Lett. **79**, 1547 (1997).

[24] N. R. Claughton and C. J. Lambert, Phys. Rev. B **53**, 6605 (1996).

[25] H. Courtois, P. Gandit, D. Mailly, and B. Pannetier, Phys. Rev. Lett. **76**, 130 (1996).

[26] A. F. Andreev, J. Exptl. Theoret. Phys. **49**, 655 (1965), [Sov. Phys. JETP **22**, 455 (1966)].

[27] I. O. Kulik, Zh. Eksp. Teor. Fiz. **57**, 1745 (1969), [Sov. Phys. JETP **30**, 944 (1970)].

[28] F. Pierre, A. Anthore, H. Pothier, C. Urbina, and D. Esteve, Phys. Rev. Lett. **86**, 1078 (2001).

[29] J. Rammer and H. Smith, Rev. Mod. Phys. **58**, 323 (1986).

[30] K. E. Nagaev and M. Büttiker, Phys. Rev. B **63**, 081301 (2001).

[31] K. E. Nagaev, Phys. Rev. B **64**, 081304 (2002).

[32] N. W. Ashcroft and N. D. Mermin, *Solid State Physics* (Saunders College Publishing, Orlando, Florida, 1976).

[33] H. Smith and H. H. Jensen, *Transport Phenomena* (Clarendon press, Oxford, 1989).

[34] K. E. Nagaev, Phys. Lett. A **169**, 103 (1992).

[35] E. V. Sukhorukov and D. Loss, Phys. Rev. B **59**, 13054 (1999).

[36] A. Schmid and G. Schön, J. Low Temp. Phys. **20**, 207 (1975).

[37] F. Pierre, *Interactions electron-electron dans les fils mesoscopiques* (Ph.D. Thesis, University of Paris 6, France, 2000).

[38] F. Pierre, H. Pothier, D. Esteve, and M. H. Devoret, J. Low Temp. Phys. **118**, 437 (2000).

[39] F. Pierre, H. Pothier, D. Esteve, M. H. Devoret, A. B. Gougam, and N. O. Birge, in *Kondo Effect and Dephasing in Low-Dimensional Metallic Systems*, edited by V. Chandrasekhar, C. van Haesendonck, and A. Zawadowski (Kluwer, Dordrecht, 2001), p. 119, e-print: [cond-mat/0012038].

[40] A. Kaminski and L. I. Glazman, Phys. Rev. Lett. **86**, 2400 (2001).

[41] J. Kroha and A. Zawadowski, Phys. Rev. Lett. **88**, 176803 (2002).

[42] R. Landauer, IBM J. Res. Dev. **1**, 223 (1957).

[43] M. Büttiker, Phys. Rev. Lett. **57**, 1761 (1986).

[44] G. Eilenberger, Z. Phys. **214**, 195 (1968).

[45] K. D. Usadel, Phys. Rev. Lett. **25**, 507 (1970).

[46] N. N. Bogoliubov, J. Exptl. Theoret. Phys. **34**, 58 (1958), [Sov. Phys. JETP **34**, 41 (1958)].

[47] P. G. de Gennes, Rev. Mod. Phys. **36**, 225 (1964).

[48] J. Bardeen, L. N. Cooper, and J. R. Schrieffer, Phys. Rev. **108**, 1175 (1957).

[49] G. E. Blonder, M. Tinkham, and T. M. Klapwijk, Phys. Rev. B **25**, 4515 (1982).

[50] R. Landauer, Philos. Mag. **21**, 863 (1970).

[51] R. Landauer, IBM J. Res. Dev. **32**, 306 (1988).

[52] M. Büttiker, IBM J. Res. Develop. **32**, 317 (1988).

[53] S. Datta, *Electronic Transport in Mesoscopic Systems* (University Press, Cambridge, 1995).

[54] T. T. Heikkilä, *Electronic transport in superconducting nanostructures: scattering approach* (Master's Thesis, Helsinki University of Technology, Finland, 1998).

[55] C. W. J. Beenakker, Phys. Rev. B **46**, 12841 (1992).

[56] C. J. Lambert, J. Phys. Condens. Matter **3**, 6579 (1991).

[57] Y. M. Blanter and M. Büttiker, Phys. Rep. **336**, 1 (2000).

[58] C. W. J. Beenakker, Rev. Mod. Phys. **69**, 731 (1997).

[59] Y. V. Nazarov, Phys. Rev. Lett. **73**, 134 (1994).

[60] K. M. Schep and G. E. W. Bauer, Phys. Rev. Lett. **78**, 30151 (1997).

[61] B. Kramer and A. MacKinnon, Rep. Prog. Phys. **56**, 1469 (1993).

[62] D. S. Fisher and P. A. Lee, Phys. Rev. B **23**, 6851 (1981).

[63] Y. Takane and H. Ebisawa, J. Phys. Soc. Jpn **61**, 1685 (1992).

[64] C. J. Lambert, V. C. Hui, and S. J. Robinson, J. Phys.: Condens. Matter **5**, 4187 (1993).

[65] P. W. Anderson, Phys. Rev. **109**, 1492 (1958).

[66] B. Kramer and A. MacKinnon, Rep. Prog. Phys. **56**, 1469 (1993).

[67] I. K. Marmorkos, C. W. J. Beenakker, and R. A. Jalabert, Phys. Rev. B **48**, 2811 (1993).

[68] Y. V. Nazarov, Phys. Rev. B **52**, 4720 (1995).

[69] W. Belzig and Y. V. Nazarov, Phys. Rev. Lett. **87**, 067006 (2001).

[70] F. Wilhelm, *Ladungstransport in supraleitenden Nanostrukturen* (Ph.D. Thesis, University of Karlsruhe, Germany, 1999).

[71] J. B. Ketterson and S. N. Song, *Superconductivity* (University Press, Cambridge, 1999).

[72] N. Kopnin, *Theory of Nonequilibrium Superconductivity* (Clarendon press, Oxford, 2001).

[73] L. P. Gorkov, Sov. Phys. JETP **7**, 505 (1958).

[74] A. A. Abrikosov, L. P. Gorkov, and I. E. Dzyaloshinski, *Methods of Quantum Field Theory in Statistical Physics* (Dover publications, Inc., New York, 1975).

[75] U. Eckern and A. Schmid, J. Low Temp. Phys. **45**, 137 (1981).

[76] S.-K. Yip, Superlatt. Microstruct. **25**, 1213 (1999).

[77] A. Shelankov and M. Ozana, Phys. Rev. B **61**, 7077 (2000).

[78] J. W. Serene and D. Rainer, Phys. Rep. **101**, 221 (1983).

[79] N. Schopol and K. Maki, Phys. Rev. B **52**, 490 (1995).

[80] A. L. Fetter and J. D. Walecka, *Quantum Theory of Many-Particle Systems* (McGraw-Hill, New York, 1971).

[81] T. Matsubara, Prog. Theor. Phys. **14**, 351 (1955).

[82] L. V. Keldysh, Zh. Eksp. Teor. Fiz. **47**, 1515 (1964), [Sov. Phys. JETP 20, 1018 (1965)].

[83] A. I. Larkin and Y. N. Ovchinnikov, Zh. Eksp. Teor. Fiz. **55**, 2262 (1968), [Sov. Phys. JETP **28**, 1200 (1968)].

[84] W. Belzig, *Magnetic and spectral properties of superconducting proximity-systems* (Ph.D. Thesis, University of Karlsruhe, Germany, 1999).

[85] S.-W. Lee, A. V. Galaktionov, and C.-M. Ryu, J. Korean Phys. Soc. **34**, S193 (1999).

[86] A. V. Zaitsev, Zh. Eksp. Teor. Fiz. **86**, 1742 (1984), [Sov. Phys. JETP **59**, 1015 (1984)].

[87] M. Y. Kuprianov and V. F. Lukichev, Zh. Eksp. Teor. Fiz. **94**, 139 (1988).

[88] Y. V. Nazarov, Superlatt. Microstruct. **25**, 1221 (1999).

[89] P. A. Lee, A. D. Stone, and H. Fukuyama, Phys. Rev. B **35**, 1039 (1987).

[90] T. Dittrich, P. Hänggi, G.-L. Ingold, B. Kramer, G. Schön, and W. Zwerger, in *Quantum Transport and Dissipation* (Wiley-VCH, Weinheim, 1997), Chap. 1.

[91] T. Mühge, N. N. Garif'yanov, Y. V. Goryunov, G. G. Khaliullin, L. R. Tagirov, K. Westerholt, I. A. Garifullin, and H. Zabel, Phys. Rev. Lett. **77**, 1857 (1996).

[92] F. S. Bergeret, K. B. Efetov, and A. I. Larkin, Phys. Rev. B **62**, 11872 (2000).

[93] W. A. Harrison, *Solid State Theory* (McGraw-Hill, New York, 1970).

[94] P. Fulde and R. A. Ferrell, Phys. Rev. **135**, A550 (1964).

[95] A. I. Larkin and Y. N. Ovchinnikov, Sov. Phys. JETP **20**, 762 (1965).

[96] M. J. M. de Jong and C. W. J. Beenakker, Phys. Rev. Lett. **74**, 1657 (1995).

[97] S. K. Upadhyay, A. Palanisami, R. N. Louie, and R. A. Buhrman, Phys. Rev. Lett. **81**, 3247 (1998).

[98] R. Mélin, Europhys. Lett. **51**, 202 (2000).

[99] E. A. Demler, G. B. Arnold, and M. R. Beasley, Phys. Rev. B **55**, 15174 (1997).

[100] F. S. Bergeret, A. F. Volkov, and K. B. Efetov, Phys. Rev. B **64**, 134506 (2001).

[101] F. S. Bergeret, A. F. Volkov, and K. B. Efetov, Phys. Rev. B **65**, 134505 (2002).

[102] A. I. Buzdin, L. N. Bulaevskii, and S. V. Panyukov, Pis'ma Zh. Eksp. Teor. Fiz. **35**, 147 (1982), [JETP Lett. **35**, 178 (1982)].

[103] R. Fazio and C. Lucheroni, Europhys. Lett. **45**, 707 (1999).

[104] V. T. Petrashov, V. N. Antonov, S. V. Maksimov, and R. S. Shaĭkhaĭdarov, JETP Lett. **59**, 551 (1994).

[105] W. Belzig, A. Brataas, and Y. V. Nazarov, Phys. Rev. B **62**, 9726 (2000).

[106] M. Giroud, K. Hasselbach, H. Courtois, D. Mailly, and B. Pannetier, preprint [cond-mat/0204140] (unpublished).

[107] M. Giroud, Private communications, 2002.

[108] J. Aumentado and V. Chandrasekhar, Phys. Rev. B **64**, 054505 (2001).

[109] F. S. Bergeret, A. F. Volkov, and K. B. Efetov, Phys. Rev. Lett. **86**, 4096 (2001).

[110] M. Fogelström, Phys. Rev. B **62**, 11812 (2000).

[111] G. Deutscher and D. Feinberg, Appl. Phys. Lett. **76**, 487 (2000).

[112] A. Frydman and R. C. Dynes, Solid State Commun. **110**, 485 (1999).

[113] V. N. Krivoruchko and E. A. Koshina, Phys. Rev. B **66**, 014521 (2002).

[114] A. I. Buzdin, B. Bujicic, and K. M. Yu., Zh. Eksp. Teor. Fiz. **101**, 231 (1992), [Sov. Phys. JETP **74**, 124 (1992)].

[115] L. N. Bulaevskii, V. V. Kuzii, and A. A. Sobyanin, JETP Lett. **25**, 290 (1977).

[116] A. V. Veretennikov, V. V. Ryazanov, V. A. Oboznov, A. Y. Rusanov, V. A. Larkin, and J. Aarts, Physica B **284-288**, 495 (2000).

[117] V. V. Ryazanov, V. A. Oboznov, A. Y. Rusanov, A. V. Veretennikov, A. A. Golubov, and J. Aarts, Phys. Rev. Lett. **86**, 2427 (2001).

[118] F. Taddei, S. Sanvito, J. H. Jefferson, and C. J. Lambert, Phys. Rev. Lett. **82**, 4938 (1999).

[119] C. P. Umbach, S. Washburn, R. B. Laibowitz, and R. A. Webb, Phys. Rev. B **30**, 4048 (1984).

[120] J. C. Licini, D. J. Bishop, M. A. Kastner, and J. Melngailis, Phys. Rev. Lett. **55**, 2987 (1985).

[121] B. L. Altshuler, Pis'ma Zh. Eksp. Teor. Fiz. **51**, 530 (1985), [JETP Lett. **41**, 648 (1985)].

[122] B. L. Altshuler and D. E. Khmelnitskii, Pis'ma Zh. Eksp. Teor. Fiz. **42**, 291 (1985), [JETP Lett. **42**, 359 (1986)].

[123] P. A. Lee and A. D. Stone, Phys. Rev. Lett. **55**, 1622 (1985).

[124] B. L. Altshuler and B. I. Shklovskii, Zh. Eksp. Teor. Fiz. **91**, 220 (1986), [JETP **64**, 127 (1986)].

[125] Y. Imry, Europhys. Lett. **1**, 249 (1986).

[126] C. W. J. Beenakker and B. Rejaei, Phys. Rev. Lett. **71**, 3689 (1993).

[127] J. T. Chalker and A. M. S. Macêdo, Phys. Rev. Lett. **71**, 3693 (1993).

[128] P. W. Brouwer and C. W. J. Beenakker, Phys. Rev. B **52**, 16772 (1995).

[129] A. Altland and M. R. Zirnbauer, Phys. Rev. B **55**, 1142 (1997).

[130] A. D. Stone, Phys. Rev. Lett. **54**, 2692 (1985).

[131] T. Kemen, T. Bauch, W. Bär, K. Hecker, A. Marx, and R. Gross, J. Low Temp. Phys. **118**, 679 (2000).

[132] S. G. den Hartog and B. J. van Wees, Phys. Rev. Lett. **80**, 5023 (1998), reply: Hecker, *et al.*, *ibid* **80**, 5024.

[133] S. G. den Hartog, C. M. A. Kapteyn, B. J. van Wees, T. M. Klapwijk, W. van der Graaf, and G. Borghs, Phys. Rev. Lett. **76**, 4592 (1996).

[134] S. G. den Hartog, C. M. A. Kapteyn, B. J. van Wees, T. M. Klapwijk, and G. Borghs, Phys. Rev. Lett. **77**, 4954 (1997).

[135] K. K. Likharev, Rev. Mod. Phys. **51**, 101 (1979).

[136] Y. Makhlin, G. Schön, and A. Shnirman, Rev. Mod. Phys. **73**, 357 (2001).

[137] I. O. Kulik and A. N. Omelyan'chuk, ZhETF Pis. Red. **21**, 216 (1974), [JETP Lett. **21**, 96 (1975)].

[138] A. D. Zaikin and G. F. Zharkov, Fiz. Nizk. Temp. **7**, 375 (1981), [Sov. J. Low Temp. Phys. **7**, 184 (1981)].

[139] B. J. van Wees, K.-M. H. Lenssen, and C. J. P. M. Harmans, Phys. Rev. B **44**, 470 (1991).

[140] A. F. Volkov, Phys. Rev. Lett. **74**, 4730 (1995).

[141] C. Ishii, Progr. Theor. Phys. **44**, 1525 (1970).

[142] S. K. Yip, Phys. Rev. B **58**, 5803 (1998).

[143] J. J. A. Baselmans, B. J. van Wees, and T. M. Klapwijk, Phys. Rev. B **63**, 094504 (2001).

[144] J. Bardeen and J. L. Johnson, Phys. Rev. B **5**, 72 (1972).

[145] A. I. Buzdin and M. Y. Kupriyanov, Pis'ma Zh. Eksp. Teor. Fiz. **53**, 308 (1991), [JETP Lett. **53**, 321 (1991)].

[146] A. F. Volkov, R. Seviour, and V. V. Pavlovskii, Superlatt. Microstruct. **25**, 647 (1999).

[147] S.-K. Yip, Phys. Rev. B **62**, R6127 (2000).

[148] E. Il'ichev, M. Grajcar, R. Hlubina, R. P. J. IJsselsteijn, H. E. Hoenig, H.-G. Meyer, A. Golubov, M. H. S. Amin, A. M. Zagoskin, A. N. Omelyanchouk, and M. Y. Kupriyanov, Phys. Rev. Lett. **86**, 5369 (2001).

[149] J. Eom, C.-J. Chien, and V. Chandrasekhar, Phys. Rev. Lett. **81**, 437 (1998).

[150] R. Seviour and A. F. Volkov, Phys. Rev. B **62**, R6116 (2000).

[151] C. J. Pethick and H. Smith, Phys. Rev. Lett. **43**, 640 (1979).

[152] J. Clarke, B. R. Fjordbøge, and P. E. Lindelof, Phys. Rev. Lett. **43**, 642 (1979).

[153] A. Schmid and G. Schön, Phys. Rev. Lett. **43**, 793 (1979).

[154] J. Clarke and M. Tinkham, Phys. Rev. Lett. **44**, 106 (1980).

[155] M. A. Nielsen and I. L. Chuang, *Quantum Computation and Quantum Information* (University Press, Cambridge, 2000).

[156] B. A. Muzykantskii and D. E. Khmelnitskii, Phys. Rev. B **50**, 3982 (1994).

[157] M. J. M. de Jong and C. W. J. Beenakker, Phys. Rev. B **49**, 16070 (1994).

[158] E. V. Sukhorukov and D. Loss, Phys. Rev. Lett. **80**, 4959 (1998).

[159] F. Lefloch, C. Hoffmann, M. Sanquer, and D. Quirion, [cond-mat/0208126] (unpublished).

[160] V. V. Ryazanov, V. A. Oboznov, A. V. Veretennikov, and A. Y. Rusanov, Phys. Rev. B **65**, 020501(R) (2001).

[161] G. Blatter, V. B. Geshkenbein, and L. B. Ioffe, Phys. Rev. B **63**, 174511 (2001).

[162] A. Altland, B. D. Simons, and D. Taras-Semchuk, JETP Lett. **67**, 22 (1998).

Abstracts of publications I–IX

I We examine universal conductance fluctuations (UCF's) in mesoscopic normal-superconducting-normal (N-S-N) structures using a numerical solution of the Bogoliubov-de Gennes equation. We discuss two cases depending on the presence ("open" structure) or absence ("closed" structure) of quasiparticle transmission. In contrast to N-S structures, where the onset of superconductivity increases fluctuations, we find that UCF's are suppressed by superconductivity for N-S-N structures. We demonstrate that the fluctuations in "open" and "closed" structures exhibit distinct responses to an applied magnetic field and to an imposed phase variation of the superconducting order parameter.

II We study differential shot noise in mesoscopic diffusive normal-superconducting (NS) heterostructures at finite voltages where nonlinear effects due to the superconducting proximity effect arise. A numerical scattering-matrix approach is adopted. Through an NS contact, we observe that the shot noise shows a reentrant dependence on voltage due to the superconducting proximity effect but the differential Fano factor stays approximately constant. Furthermore, we consider differential shot noise in the structures where an insulating barrier is formed between normal and superconducting regions and calculate the differential Fano factor as a function of barrier height.

III We examine the influence of the superconducting proximity effect on the thermoelectric response of hybrid mesoscopic normal metal - superconductor nanostructures. We demonstrate that Andreev scattering can break the well-known Mott relation between the thermopower and the logarithmic energy derivative of the conductance. We also consider the effect of superconductivity on the temperature dependence of the thermopower.

IV We study the electronic density of states in a mesoscopic superconductor near a transparent interface with a ferromagnetic metal. In our tunnel spectroscopy experiment, a substantial density of states is observed at sub-gap energies close to a ferromagnet. We compare our data with detailed calculations based on the Usadel equation, where the effect of the ferromagnet is treated as an effective boundary condition. We achieve an excellent agreement with theory when non-ideal quality of the interface is taken into account.

V We consider a mesoscopic normal metal, where the spin degeneracy is lifted by a ferromagnetic exchange field or Zeeman splitting, coupled to two superconducting reservoirs. As a function of the exchange field or the distance between the reservoirs, the supercurrent through this device oscillates with an exponentially decreasing envelope. This phenomenon is similar to the tuning of a supercurrent by a non-equilibrium quasiparticle distribution between two voltage-biased reservoirs. We propose a device combining the exchange field and non-equilibrium effects, which allows us to observe a range of novel phenomena. For instance, part of the field-suppressed supercurrent can be recovered by a voltage between the additional probes.

VI Recently Baselmans et al. [Nature, (London) **397**, 43 (1999)] showed that the direction of the supercurrent in a superconductor/normal/superconductor Josephson junction can be reversed by applying, perpendicularly to the supercurrent, a sufficiently large control current between two normal reservoirs. The unusual behavior of their 4-terminal device (called a controllable junction) arises from the nonequilibrium electron energy distribution established in the normal wire between the two superconductors. We have observed a similar supercurrent reversal in a 3-terminal device, where the control current passes from a single normal reservoir into the two superconductors. We show theoretically that this behavior, although intuitively less obvious, arises from the same nonequilibrium physics present in the 4-terminal device. Moreover, we argue that the amplitude of the -state critical current should be at least as large in the 3-terminal device as in a comparable 4-terminal device.

VII Recent experiments have demonstrated the nonequilibrium control of the supercurrent through diffusive phase-coherent normal-metal weak links. The experimental results have been accurately described by the quasiclassical Green's function technique in the Keldysh formalism. Taking into account the geometry of the structure, different energy scales and the nonidealities at the interfaces allows us to obtain a quantitative agreement between the theory and the experimental results in both the amplitude and the phase dependence of the supercurrent, with no or very few fitting parameters. Here we discuss the most important factors involved with such comparisons: the ratio between the superconducting order parameter and the Thouless energy of the junction, the effect of additional wires on the weak link, and the effects due to imperfections, most notably due to the nonideal interfaces.

VIII We measure the full supercurrent-phase relation of a controllable π junction around the transition from the conventional 0 state to the π state. We show that around the transition the Josephson supercurrent-phase relation changes from $I_{\rm sc} \simeq I_c \sin(\varphi)$ to $I_{\rm sc} \simeq I_c \sin(2\varphi)$. This implies that, around the transition, two minima in the junction free energy exist, one at $\varphi = 0$ and one at $\varphi = \pi$ whereas only one minimum exists at the 0 state (at $\varphi = 0$) and at the π state (at $\phi = \pi$). Theoretical calculations based on the quasiclassical theory are in good agreement with the observed behavior.

IX The local nonequilibrium quasiparticle distribution function in a normal-metal wire depends on the applied voltage over the wire and the type and strength of different scattering mechanisms. We show that in a setup with superconducting reservoirs, in which the supercurrent and the dissipative current flow (anti)parallel, the distribution function can also be tuned by applying a supercurrent between the contacts. Unlike the usual control by voltage or temperature, this leads to a Peltier-like effect: the supercurrent converts an externally applied voltage into a difference in the effective temperature between two parts of the system maintained at the same potential. We suggest an experimental setup for probing this phenomenon and mapping out the controlled distribution function.

ISBN 951-22-6187-1
ISSN 1456-3320